Acta Crystallographica Section B
Structural Science
ISSN 0108-7681

Structure refinement and superspace description of the system $Bi_{2(n+2)}Mo_nO_{6(n+1)}$ (n = 3, 4, 5 and 6)

P. J. Bereciartua,[a]* F. J. Zuñiga,[a] J. M. Perez-Mato,[a] V. Petříček,[b] E. Vila,[c] A. Castro,[c] J. Rodríguez-Carvajal[d] and S. Doyle[e]

[a]Department of Condensed Matter Physics, University of the Basque Country, Bilbao, Spain, [b]Institute of Physics of the Academy of Sciences of the Czech Republic, Praha, Czech Republic, [c]Instituto de Ciencia de Materiales de Madrid (ICMM, CSIC), Madrid, Spain, [d]Institut Laue–Langevin, Grenoble, France, and [e]Institute for Synchrotron Radiation (ISS), ANKA, Forschungszentrum Karlsruhe GmbH, Eggenstein-Leopoldshafen, Germany

Correspondence e-mail: pjbereciartu001@ehu.es

Received 10 January 2012
Accepted 19 April 2012

B-IncStrDB Reference: 6402ESgKUu

The system $Bi_{2(n+2)}Mo_nO_{6(n+1)}$ is described within the superspace formalism. Two superspace models are proposed for the different members of this family, depending on the parity of the parameter n. The superspace model for the odd members is constructed through the embedding of the cationic distribution of the member with $n = 3$, and the modification of a superspace model previously proposed for the compound Bi_2MoO_6. However, this model cannot be applied to the even members of the family. Performing the appropriate transformations, a suitable superspace model for the even members is obtained. The atomic structure of the different compounds of the family have been refined through the Rietveld method combining synchrotron X-ray and neutron powder diffraction data.

1. Introduction

Due to the functional properties of some compounds obtained within the Bi_2O_3–MoO_3 system, mainly catalysts (Galvan *et al.*, 1993; Agarwal *et al.*, 1994) and good ionic conductors (Vannier *et al.*, 2000; Galy *et al.*, 2006; Holmes *et al.*, 2008), this binary system has been extensively studied. Within this context, four new compounds, $Bi_{10}Mo_3O_{24}$, $Bi_6Mo_2O_{15}$, $Bi_{14}Mo_5O_{36}$ and $Bi_8Mo_3O_{21}$, have been found in the mBi_2O_3–MoO_3 system, corresponding to m = 1.666, 1.500, 1.400 and 1.333 (Vila *et al.*, 2004, 2005, 2007). Samples synthesized within the range of composition $1.0 < m < 1.7$ were studied and characterized by powder X-ray diffraction and transmission electron microscopy, confirming the existence of the above-mentioned single phases and a mixture of phases for intermediate compositions. These compounds can be considered as members of the series $Bi_{2(n+2)}Mo_nO_{6(n+1)}$ with n = 3, 4, 5 and 6. The two end-members of this series are the well known Bi_2O_3 (for $n = 0$) and Bi_2MoO_6 (for $n = \infty$). The structure of the different compounds of this system are related to that of fluorite, except for the end Mo-rich member, Bi_2MoO_6, that exhibits an Aurivillius-type structure. Lattice parameters and space groups are summarized in Table 1 of Vila *et al.* (2007) and references therein.

The crystal structure of the $n = 3$ member, *i.e.* $Bi_{10}Mo_3O_{24}$, was determined by Galy *et al.* (2009) following a multi-technique approach. The cationic Bi and Mo distribution was established with the help of high-resolution transmission electron microscopy (HRTEM) images. Assuming some crystal chemistry hypotheses, a structural model was built within the space group $C2$ and refined through the Rietveld method combining X-ray and neutron powder diffraction (XPD and NPD) data. The structure can be described as a stacking of puckered $[Bi_{10}O_{12}]$ layers parallel to the (010) plane, combined with groups of three isolated $\{MoO_4\}$ tetra-

Table 1
Experimental details corresponding to the different compounds of the system $Bi_{2(n+2)}Mo_nO_{6(n+1)}$.

Member	$n = 3$	$n = 4$	$n = 5$	$n = 6$
Crystal data				
Chemical formula	$Bi_{10}Mo_3O_{24}$	$Bi_6Mo_2O_{15}$	$Bi_{14}Mo_5O_{36}$	$Bi_8Mo_3O_{21}$
M_r	2761.60	1685.74	3981.38	2295.64
Crystal system, space group	Monoclinic, $C2$	Monoclinic, $P2_1/a$	Monoclinic, $C2$	Monoclinic, $P2_1/a$
Temperature (K)	295	295	295	295
a, b, c (Å)	23.72316 (5), 5.64745 (1), 8.68034 (2)	29.0708 (1), 5.64841 (2), 8.66155 (4)	34.4733 (2), 5.64098 (3), 8.64528 (5)	39.9117 (5), 5.63012 (6), 8.63676 (9)
β (°)	95.8734 (1)	97.9832 (2)	99.6966 (3)	100.9773 (7)
V (Å^3)	1156.847 (4)	1408.477 (9)	1657.17 (2)	1905.23 (4)
Z	2	4	2	4
X-ray data collection				
Specimen mounting	Standard holder	Standard holder	Standard holder	Standard holder
Data collection mode	Reflection	Reflection	Reflection	Reflection
Scan method	Step	Step	Step	Step
2θ values (°)	5, 35, 0.003	5, 35, 0.003	5, 35, 0.003	5, 35, 0.003
(max/min/step)	35, 65.5, 0.005	35, 65.5, 0.005	35, 65.5, 0.005	35, 65.5, 0.005
Wavelength (Å)	0.91846	0.91846	0.91846	0.91846
Neutron data collection				
Specimen mounting	Vanadium can (ø = 8 mm)	Vanadium can (ø = 8 mm)	Vanadium can (ø = 8 mm)	Vanadium can (ø = 8 mm)
Data collection mode	Transmission	Transmission	Transmission	Transmission
Scan method	Step	Step	Step	Step
2θ values (°) (max/min/step)	0, 159.95, 0.05	0, 159.95, 0.05	0, 159.95, 0.05	0, 159.95, 0.05
Wavelength (Å)	2.39968 (3)	2.39979 (7)	2.39973 (5)	2.4004 (1)

hedra. With this model and the geometric relation between the cells of the different members of the series, an extension of the same structural model to the whole family was proposed. According to this model, the $n = 5$ member keeps the same $C2$ space group with five tetrahedral units, while members with $n = 4$ and $n = 6$ present an arrangement of four and six tetrahedra with the space group $P2_1/a$.

More details about the cationic skeleton were reported by Landa-Cánovas *et al.* (2009), based on HRTEM images of members with n = 4, 5 and 6. Simulated HRTEM images performed with heavy-atom models match the experimental images, supporting the proposed cation framework. Moreover, the authors reinterpret the diffraction patterns assuming for even members (n = 4 and 6) a different a parameter whose value is half the original one proposed by Vila *et al.* (2007) and assign the space group $P2_1$ to these two phases. Since the new a parameter and space group of n even phases are only justified by the model of cations, it is very plausible that the entire structure with the O atoms corresponds to another cell and space group. In any case, the regularities of the proposed cationic array suggest that this model will exist for all members, even those which have not been experimentally observed (n = 1 and 2). As pointed out by Landa-Cánovas *et al.* (2009), the case with $n = \infty$ (Bi_2MoO_6) could seem inconsistent with the above statement as its Aurivillius-type structure (van den Elzen & Rieck, 1973) consists of $\{MoO_6\}$ corner-sharing octahedral layers periodically stacked with Bi_2O_3 layers. However, the connection between the two types of structures can be found if we consider that a shift of Mo atoms towards an equatorial edge of the octahedra transforms these units into isolated tetrahedra. The transition between the Aurivillius-type structure and the cationic array of any member of the series is established through a crystallographic shear breaking the $[Bi_2O_2]$ layer to accommodate the additional Bi_2O_3 that fits the composition of the member. This mechanism applied to every three, four, five or six $\{MoO_6\}$ units leads to the corresponding structural model for each member of the series (Figs. 6 and 7 in Landa-Cánovas *et al.*, 2009).

The relationship between the unit-cell parameters of this series of compounds and the fluorite unit cell becomes clear through the electron diffraction pattern obtained for each phase (Vila *et al.*, 2007). As an example, the $(h\,0\,l)$ section of the weighted reciprocal space for member $n = 3$ is represented in Fig 1. The diffraction pattern can be described as consisting of two types of Bragg peaks, main and superstructure reflections. Main reflections, usually stronger than the rest, can be clearly identified and described with the basic fluorite-type reciprocal cell. Considering the corresponding reciprocal vectors $\{\mathbf{a}_F^*, \mathbf{b}_F^*, \mathbf{c}_F^*\}$, the following structural relationship can be established between the actual and the basic cells (Vila *et al.*, 2007)

$$\begin{pmatrix} \mathbf{a} \\ \mathbf{b} \\ \mathbf{c} \end{pmatrix} = \begin{pmatrix} n+1 & 0 & 1 \\ 0 & 1 & 0 \\ -\frac{1}{2} & 0 & \frac{3}{2} \end{pmatrix} \begin{pmatrix} \mathbf{a}_\mathrm{F} \\ \mathbf{b}_\mathrm{F} \\ \mathbf{c}_\mathrm{F} \end{pmatrix}, \qquad (1)$$

where n = 3, 4, 5 and 6 refers to each member of the family. The remaining weak reflections can be indexed as superstructure reflections of the basic fluorite cell.

An alternative description of the diffraction patterns in the context of the superspace crystallography requires the consideration of the main reflections as associated with a basic cell (fluorite type), and the superstructure reflections as satellite reflections due to a modulation wavevector **q**.

According to this scheme, each Bragg peak of the diffraction pattern can be indexed with a reciprocal vector

$$\mathbf{H} = h\mathbf{a}_F^* + k\mathbf{b}_F^* + l\mathbf{c}_F^* + m\mathbf{q}, \quad (2)$$

where $\mathbf{q}$ is the modulation vector. The regularity observed in the diffraction patterns of the series of compounds allowed Vila *et al.* (2007) to propose a modulation vector different for each compound, given by

$$\mathbf{q}_V = \frac{1}{3n+4}(6\mathbf{a}_F^* + 2\mathbf{c}_F^*). \quad (3)$$

Since all members of the family present the same set of main reflections and a modulation vector $\mathbf{q}_V$ specific to each compound, it is expected that these phases can be described through a superspace model. This approach has already been successfully applied to other systems with flexible composition-like systems A_xBX_3 derived from the hexagonal perovskite structure (Evain *et al.*, 1998), the composites $A_{1+x}(A'_xB_{1-x})O_3$ (Perez-Mato *et al.*, 1999), the intergrowth polytypes of the system $LaTi_{1-x}O_3$ (Elcoro *et al.*, 2000) or the series $A_nB_nO_{3n+2}$ (Elcoro *et al.*, 2001). This last model has been successfully applied to the $n = 4$ member of the series $(Na,Ca)_nNb_nO_{3n+2}$ (Elcoro *et al.*, 2004) and the members $n = 5$ and 6 of the homologous series $Ca_n(Nb,Ti)_nO_{3n+2}$ (Guevarra *et al.*, 2007). In this context, each compound of the series is described as a different distortion or modulation of a common average structure.

In the present work we apply this approach to describe the structure of the whole series by means of the superspace formalism. Through the embedding of the three-dimensional cationic distribution proposed for the $n = 3$ member, a convenient modulation vector has been chosen. Considering the unit cell of the fluorite structure and this modulation vector, a superspace model has been constructed from the Aurivillius-type structure of the end-member Bi_2MoO_6. However, this superspace model cannot be applied to even members, since it leads to an incorrect three-dimensional unit cell. Some modifications are required to build the corresponding model for even members. As a result, the compounds of the family $Bi_{2(n+2)}Mo_nO_{6(n+1)}$ are described through two different superspace models, depending on the parity of the parameter n. The atomic structures of the different compounds have been refined and the superspace models have been checked by the Rietveld method combining X-ray powder diffraction (XPD) and neutron powder diffraction (NPD) data.

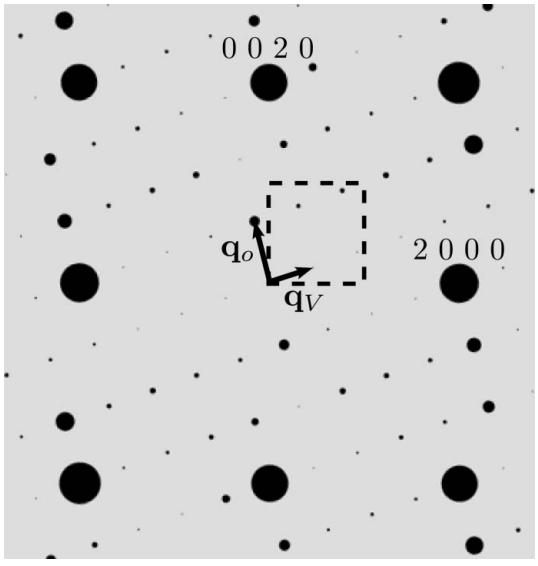

Figure 1
Section $(h\,0\,l)$ of the weighted reciprocal space of the member with $n = 3$. It corresponds to the $(h\,0\,l\,m)$ section within the superspace approach. Main reflections ($m = 0$) are related with the reciprocal unit cell of the fluorite structure (dashed line). Two possible modulation vectors to index satellite reflections are indicated ($\mathbf{q}_V$ and $\mathbf{q}_o$). Note the fluorite F-centred extinction.

2. Experimental

Samples of the compounds $Bi_{10}Mo_3O_{24}$ ($n = 3$), $Bi_6Mo_2O_{15}$ ($n = 4$), $Bi_{14}Mo_5O_{36}$ ($n = 5$) and $Bi_8Mo_3O_{21}$ ($n = 6$) were synthesized through the wet-chemistry method described by Vila *et al.* (2004).

The XPD data were obtained on the PDIFF beamline at the ANKA Synchrotron Light Source in Karlsruhe. The measurements were carried out in Bragg–Brentano geometry with a wavelength of $\lambda = 0.91846$ Å at room temperature. In order to optimize peak resolution and counting statistics, the diffraction patterns were collected in two stages. For 2θ between 5 and 35° an angular step of 0.003° was employed with a counting time of 0.5 s per step; for 2θ between 35 and 65.5° a larger angular step of 0.005° was used with a longer counting time of 1 s per step. Each measurement was repeated twice in order to improve counting statistics. The data were normalized with the monitor counting rates.

The NPD data were measured on the high-resolution diffractometer D2B at the Institute Laue–Langevin in Grenoble. The experiments were carried out in Debye–Scherrer geometry with a wavelength $\lambda = 2.39970$ (3) Å from a Ge(331) monochromator. The data were collected within an angular range of 2θ between 0 and 159.95° in steps of 0.05°. Full diffraction profiles were measured with counting times of 5 h at room temperature.

Indexing the XPD patterns with the reported lattice parameters reveals the presence of a few unindexed lines which do not correspond to the studied phases. The low intensities of these peaks make the identification of the unknown phase difficult, although the starting materials of the synthesis were ruled out. The X-ray diffraction patterns also exhibit a small amount of amorphous compound which has been included in the modelled background. Moreover, the X-ray diffraction patterns contain a common unidentified peak that has been removed excluding a small region of the diffraction pattern. In the X-ray diffraction pattern of the $n = 5$ member another unidentified peak at low angles has also been excluded. The sample corresponding to the $n = 4$ member also contains a certain amount of the compound $Bi_{14}Mo_5O_{36}$ ($n = 5$).

Table 2
Background-corrected reliability factors obtained with the XPD and NPD patterns of the $n = 3$ member using the three-dimensional and superspace models.

	Three-dimensional model		Superspace model	
	XPD	NPD	XPD	NPD
R_p	0.1253	0.1075	0.1254	0.1073
R_{wp}	0.1451	0.1104	0.1452	0.1106
S	1.23	1.97	1.23	1.98
R_B(all)	0.0359	0.0429	0.0359	0.0421
R_F(all)	0.0212	0.0283	0.0213	0.0281
No. of parameters	79	76	78	75

Experimental details of the different data sets are summarized in Table 1.

3. Member with n = 3

All structural refinements were performed with the software package *JANA*2006 (Petříček *et al.*, 2006). This program allows us to combine multiple data sets from X-ray and neutron diffraction experiments to refine three-dimensional and superspace models. Within this last approach, occupational modulation can be described by crenel or sawtooth functions, which can be combined with displacive modulations represented by the sum of harmonic or Legendre polynomial series. Several of these features are used in this study.

In the refinement process the data blocks were combined with no additional weighting factors. According to the scheme used by the program *JANA*2006, the weight of each data point is only based on the value of the corresponding $\sigma(I)$ experimentally obtained.

3.1. Refinement of the three-dimensional structure

Prior to the construction of the superspace models, the three-dimensional structure determined for the $n = 3$ member by Galy *et al.* (2009) has been refined through the Rietveld method employing the XPD and NPD data simultaneously. Agreement between observed and calculated patterns for both X-ray and neutron diffraction data is presented in Fig. S1 of the supplementary material[1] and the final reliability factors, given in Table 2, confirm the quality of the experimental data. The three-dimensional structure is represented in Fig. 2. Details of this structure are given in the deposited CIF file. The refined atomic coordinates, which hardly differ from the original ones, were used for the construction of the superspace model.

3.2. Choice of the average unit cell and the modulation vector

In general, the superspace formalism makes it possible to construct a superspace model through the embedding of a given three-dimensional structure. This process assigns a point within the superspace unit cell to each atomic position in three-dimensional space, thus allowing the definition of the atomic domains like strings which represent atoms in superspace formalism. A graphical representation of the embedding process is illustrated in Fig. 3. For the embedding process only an average unit cell and a modulation vector are required. Thus, the embedding of the cation distribution of the member with $n = 3$ makes it possible to conveniently choose the average unit cell and the modulation vector. Note that different sections of the same superspace model are distinguished by the t parameter.

From the atomic distribution represented in Fig. 2, a face-centred unit cell can be assumed for the description of the positions of the cations. With this basic cell, all cations are associated with the same average position and the embedding process implies certain order along internal space. In super-

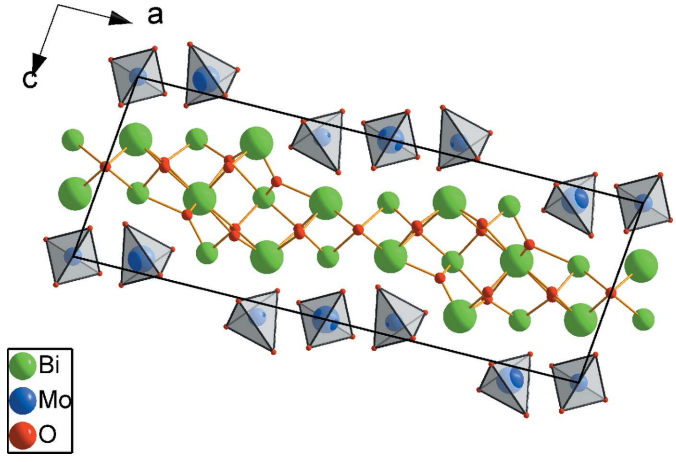

Figure 2
Projection along the **b** axis of the three-dimensional structure of the $n = 3$ member. Bi and Mo atoms are located at $y \simeq 0$ (small spheres) and $y \simeq \frac{1}{2}$ (large spheres).

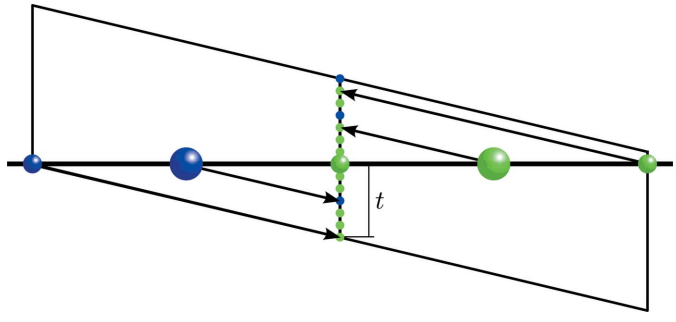

Figure 3
Embedding of the three-dimensional cationic distribution in superspace. Using the three-dimensional unit cell of the average structure and the modulation vector $\mathbf{q}_V$, the superspace lattice can be reconstructed, since the three-dimensional space is a section of the $(3 + 1)$-dimensional superspace perpendicular to the $\mathbf{a}_{s4}$ direction. Applying the translational symmetry of the superspace lattice Σ (arrows), each atom can be associated with a point within the superspace unit cell. Note that atoms represent a row of cations along the horizontal direction as shown in the projection of Fig. 2. Bi (green) and Mo (blue) atoms are located at $y \simeq 0$ (small spheres) and $y \simeq \frac{1}{2}$ (large spheres).

[1] Supplementary data for this paper are available from the IUCr electronic archives (Reference: SN5110). Services for accessing these data are described at the back of the journal.

space formalism, this ordering is represented by the corresponding occupational modulation. Different modulation vectors will lead, in general, to different ordering along internal space. Considering the different ordering obtained, a suitable modulation vector can be chosen. The embedding of the three-dimensional cation distribution of Fig. 2 performed with the modulation vector $\mathbf{q}_V$ results in the order along internal space which is shown in Fig. 4(*a*). Note that cations are distributed in six segments (crenels): three for Mo atoms (blue) and three for Bi atoms (green). A more simple ordering along internal space can be achieved employing the alternative modulation vector $\mathbf{q}_o = \frac{1}{13}(-2\mathbf{a}_F^* + 8\mathbf{c}_F^*)$ indicated in Fig. 1. The embedding with this wavevector gives rise to an ordering of the cations which can be represented by only two complementary crenel functions, one for each type of atom, as shown in Fig. 4(*b*). In the superspace description, a crenel function only requires two parameters: one for the centre along the x_4 direction (x_4^0) and the other for the width of the atomic domain (Δ). In our case, the obtained crenel functions are given by the pairs $x_4^0 = 0$ and $\Delta = \frac{3}{13}$ for the Mo atomic domain and $x_4^0 = \frac{1}{2}$ and $\Delta = \frac{10}{13}$ for the Bi atomic domain (Fig. 4*c*). Therefore, the modulation vector $\mathbf{q}_o$ allows a very succinct description of the cation distribution.

This vector $\mathbf{q}_o$ can be expressed as a function of the n parameter, considering its relation with the modulation vector $\mathbf{q}_V$. This relation can be inferred from the diffraction patterns of the different members of the family [Fig. 1 and equation (3)]

$$\mathbf{q}_o = \frac{1}{3n+4}(-2\mathbf{a}_F^* + 2(n+1)\mathbf{c}_F^*). \qquad (4)$$

During the embedding process of the cation distribution, the symmetry group of the superspace model can also be determined. The resulting distribution obtained for the cations within the superspace unit cell together with the displacements associated with each of these atoms points out that the superspace group is $F2(\alpha 0\gamma)$, which is equivalent to the standard group $B2(\alpha 0\gamma)$ (No. 5.1 in *International Tables for Crystallography*; Janssen *et al.*, 2004). The face-centred unit cell has been maintained to show the connection with the fluorite-type structure of the compound δ-Bi_2O_3. Since the three-dimensional structure is a commensurate superstructure of the basic one, only a finite number of points within the crenels are relevant along the internal coordinate x_4. These relevant points are determined by fixing a value for the t parameter, specifying which section of the superspace model represents the three-dimensional structure. To recover a three-dimensional atomic distribution with a Mo cation located at a twofold axis (Fig. 2), it is necessary to consider $t = 0$ or any of its equivalent values.

3.3. Construction of the superspace model

As stated above, the two end-members of the system $Bi_{2(n+2)}Mo_nO_{6(n+1)}$ are the compounds Bi_2O_3 and Bi_2MoO_6 (with $n = 0$ and ∞). Any of them can be considered as the reference structure for the construction of the superspace model of this family. As will be shown in §7, the most convenient option is to describe the studied phases as different distortions of the compound Bi_2MoO_6. However, the superspace model could also be based on the fluorite-type structure of the phase δ-Bi_2O_3, and, for the sake of completeness, the construction of this alternative model has been explained in the supplementary material.

The end-member Bi_2MoO_6 ($n = \infty$) is reported to have a space group $Pca2_1$ (van den Elzen & Rieck, 1973) with a structure close to the ideal Aurivillius structure. The Aurivillius family are layered bismuth oxides whose structure is described as the regular stacking of $[M_2O_2]$ slabs (usually M = Bi) and $[A_{n-1}B_nO_{3n+1}]$ perovskite blocks. In fact, Aurivillius phases have been described within the superspace formalism as cation-deficient perovskites of the formula $AB_{1-\gamma}O_3$ within the range $0 < \gamma < \frac{1}{2}$ (Boullay *et al.*, 2002*a*,*b*). In this model the average unit-cell parameters (approximately 5.6, 5.6 and 8 Å) are related to the parameter a_p of the perovskite unit cell ($\sqrt{2}a_p$, $\sqrt{2}a_p$ and $2a_p$) and the modulation vector is $\mathbf{q} = \gamma\,\mathbf{c}_A^*$. According to this description, Bi_2MoO_6 can be characterized as a modulated structure with $\gamma = \frac{1}{2}$. Indeed, the reported structure of Bi_2MoO_6 is very close to the ideal Aurivillius structure obtained through this superspace model. The superspace group of this model is $X2cm(00\gamma)000$ with centring vectors $(\frac{1}{2}\frac{1}{2}\frac{1}{2}0)$, $(\frac{1}{2}00\frac{1}{2})$ and $(0\frac{1}{2}\frac{1}{2}\frac{1}{2})$, and symmetry operations $(x_1x_2x_3x_4)$, $(x_1 - x_2 - x_3 - x_4)$, $(x_1 - x_2\,\frac{1}{2} + x_3x_4)$ and $(x_1x_2\,\frac{1}{2} - x_3 - x_4)$. The atomic domains of this model are given in Table 3. Atomic domains of Bi, Mo and O1 present occupational modulations given by crenel functions, while the average position of the O2 atomic domain is fully occupied. Appropriate modifications of this model allow the superspace description of the system $Bi_{2(n+2)}Mo_nO_{6(n+1)}$.

The distribution of Bi and Mo atomic domains in the superspace cell is shown in Fig. 5(*a*). In the real structure, atoms deviate from the ideal positions of the basic structure. In fact, together with the mentioned occupational modula-

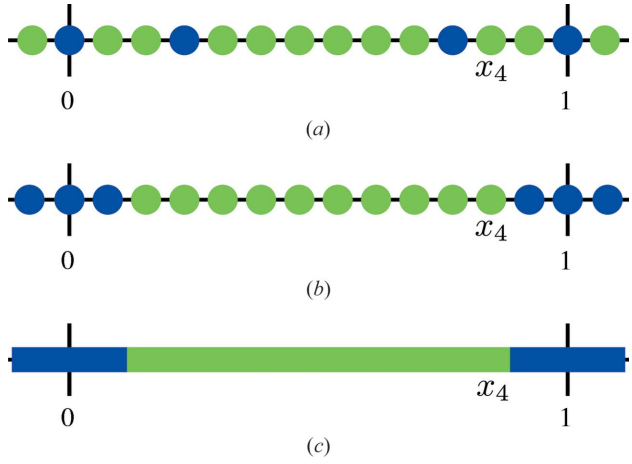

Figure 4
Occupational modulation at the cationic position. Superspace embedding gives rise to certain order along internal space (x_4 coordinate) for the Mo (blue) and Bi (green) atoms. Two different orderings are obtained with modulation vectors (*a*) $\mathbf{q}_V$ and (*b*) $\mathbf{q}_o$. The second one allows a simple description with two complementary crenel functions (*c*).

tions, atomic domains of the cations also present displacive modulations which can be modelled by sawtooth functions. This type of function represents an occupational modulation, as a crenel function, combined with a linear positional modulation, which is defined by the displacive modulation at the end of the atomic domain, given by the vector $\mathbf{u} = (u_x, u_y, u_z)$. In this case, in order to obtain the f.c.c. (face-centered cubic) cation distribution assumed for these compounds (Landa-Cánovas *et al.*, 2009), sawtooth functions for Bi and Mo atomic domains should be introduced with slopes along x_3 coordinates $u_z = \frac{1}{6}$ and $u_z = \frac{1}{12}$, as shown in Fig. 5(*b*). With the inclusion of these positional modulations, the resulting cationic atomic domains are aligned along the superspace direction [0 0 1 2], giving rise to an ordering along this direction which is equivalent to the occupational modulation obtained for the Bi and Mo atomic domains with the embedding of the three-dimensional cation distribution (Fig. 4*c*). As shown in Fig. 5(*b*), a suitable transformation of the superspace unit cell leads to a superspace model with the same distribution of cation atomic domains. The indicated transformation is given by the matrix

$$\begin{pmatrix} \mathbf{a}^{\rm F}_{s1} \\ \mathbf{a}^{\rm F}_{s2} \\ \mathbf{a}^{\rm F}_{s3} \\ \mathbf{a}^{\rm F}_{s4} \end{pmatrix} = \begin{pmatrix} 1 & 0 & 0 & 0 \\ 0 & 1 & 0 & 0 \\ 0 & 0 & 1 & 1 \\ 0 & 0 & -\frac{1}{2} & -1 \end{pmatrix} \begin{pmatrix} \mathbf{a}^{\rm A}_{s1} \\ \mathbf{a}^{\rm A}_{s2} \\ \mathbf{a}^{\rm A}_{s3} \\ \mathbf{a}^{\rm A}_{s4} \end{pmatrix}, \qquad (5)$$

where $\{\mathbf{a}^{\rm A}_{si}\}$ and $\{\mathbf{a}^{\rm F}_{si}\}$ are the basis vectors of the average unit cells related to Aurivillius and fluorite structures.

According to the proposed transformation, the new reciprocal unit cell of the average structure is given by

Table 3
Distribution of the atomic domains for the description of the compound Bi_2MoO_6 as a modulated structure of the system $AB_{1-\gamma}O_3$ with $\gamma = \frac{1}{2}$.

The average position of the O2 atom is fully occupied and the rest are represented by crenel functions. The superspace group of this model is $X2cm(00\gamma)000$ with average unit-cell parameters $a_{\rm A} \simeq 5.6$, $b_{\rm A} \simeq 5.6$ and $c_{\rm A} \simeq 8$ Å. The modulation vector is $\mathbf{q}_{\rm A} = \frac{1}{2}\mathbf{c}^*_{\rm A}$.

Atom	Average position	x_4^0	Δ
Bi	(0 0 $\frac{1}{4}$)	$\frac{1}{2}$	$\frac{1}{2}$
Mo	(0 0 0)	0	$\frac{1}{2}$
O1	(0 0 $\frac{1}{4}$)	0	$\frac{1}{2}$
O2	($\frac{1}{4}$ $\frac{1}{4}$ 0)	–	–

$$\begin{aligned} \mathbf{a}^*_{\rm F} &= \mathbf{a}^*_{\rm A} \\ \mathbf{b}^*_{\rm F} &= \mathbf{b}^*_{\rm A} \\ \mathbf{c}^*_{\rm F} &= 2\mathbf{c}^*_{\rm A} - \mathbf{q}_{\rm A} = \frac{3}{2}\mathbf{c}^*_{\rm A}, \end{aligned} \qquad (6)$$

where the subscripts F and A refer to the unit cells associated with the fluorite and Aurivillius structures. In fact, the reciprocal unit cells of both average structures can be identified in the diffraction pattern of the compound Bi_2MoO_6 (as shown in Fig. 6). The set of main reflections related to the reciprocal unit cell of the fluorite structure can be clearly recognized.

Since the unit-cell parameters of the starting superspace model are approximately 5.6, 5.6 and 8 Å, this transformation implies a new average structure with parameters 5.6, 5.6 and 5.3 Å, which agree with the unit cell employed in the embedding of the cationic distribution. This transformation also implies a new modulation vector

$$\mathbf{q}_{\rm F} = 2\mathbf{c}^*_{\rm A} - 2\mathbf{q}_{\rm A} = \mathbf{c}^*_{\rm A} = \frac{2}{3}\mathbf{c}^*_{\rm F}, \qquad (7)$$

which corresponds to the limit for $n = \infty$ of the modulation vector $\mathbf{q}_{\rm o}$ previously used [see equation (4)].

Note that the new vector $\mathbf{a}^{\rm F}_{s4} = -\frac{1}{2}\mathbf{a}^{\rm A}_{s3} - \mathbf{a}^{\rm A}_{s4}$ does not represent a symmetry translation in the superspace group of the initial model of Aurivillius phases, so the proposed transformation is not simply a change of setting of the superspace unit cell. Assuming $\mathbf{a}^{\rm F}_{s4} = -\frac{1}{2}\mathbf{a}^{\rm A}_{s3} - \mathbf{a}^{\rm A}_{s4}$ implies the inclusion of this translation in the superspace group of the new model. As a result, the distribution of the cationic atomic domains is the same as that obtained with the embedding of the Bi and Mo distribution, as was intended.

The oxygen atomic domains have also been transformed with

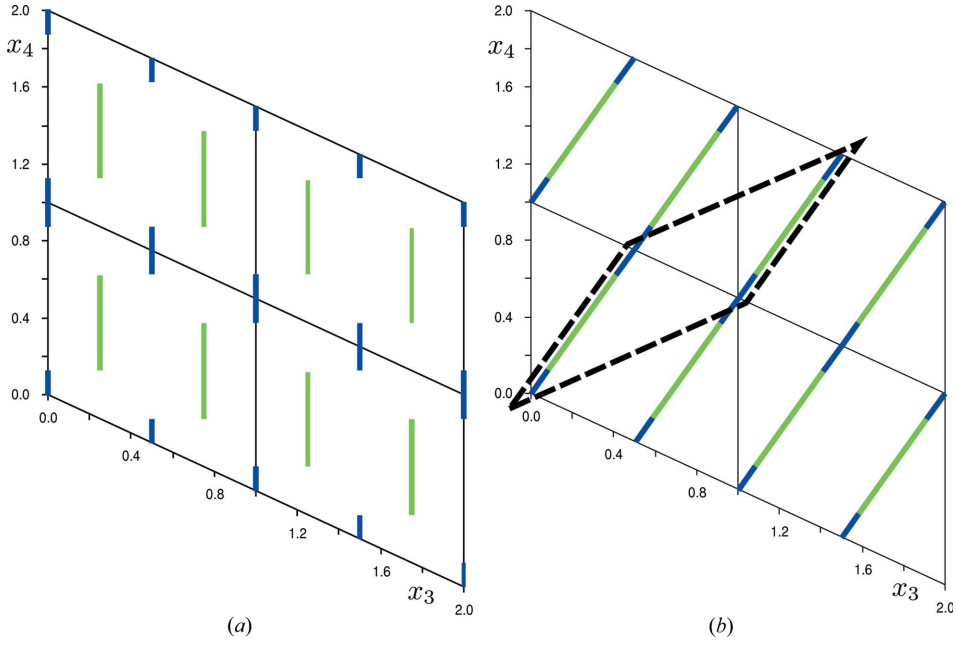

Figure 5
Distribution of the Bi (blue) and Mo (green) atomic domains in the initial model of the Aurivillius structure (*a*) and with the indicated sawtooth functions (*b*). These positional modulations give rise to the f.c.c. cationic distribution. The obtained Bi and Mo atomic domain distribution along the [0 0 1 2] direction is equal to the occupational modulation of the cations obtained through embedding (Fig. 4*c*). The new superspace unit cell is indicated by a dashed line.

this change of superspace unit cell, as shown in Fig. 7(*a*). However, these atomic domains might be described in a more suitable way, considering the neighbour cations to obtain O atomic domains associated with either Bi or Mo environments. On one hand, the O1 atom can be divided into two domains and, since they are equivalent by symmetry, it is only necessary to consider a new atom at the average position $(00\frac{3}{8})$ with a crenel function of width $\Delta = \Delta(\mathrm{Mo})$ and centre coordinate x_4^0 given by the equation

$$x_4^0 = t^0 + \mathbf{q}\cdot\bar{\mathbf{r}}^0, \tag{8}$$

where t^0 is the value of the t parameter for the centre of the atomic domain and $\bar{\mathbf{r}}^0$ is the average position. This atomic domain is the O1 atom of the new model and is related to the Mo coordination environments. Note that equation (7) restricts refinable parameters x_4^0 and $\bar{\mathbf{r}}^0$. The parameter t^0 is determined by the relative positions of this atomic domain with respect to the Mo atom (see Fig. 7*b*). Since the upper limits of these two atomic domains are given by the same t section and the widths of their crenel functions are equal, it can be concluded that $t^0(\mathrm{O1}) = t^0(\mathrm{Mo})$. On the other hand, the transformed O2 atom is located at the average position $(\frac{1}{4}\frac{1}{4}\frac{1}{4})$ and its internal space is parallel to the superspace direction [0 0 1 2], as shown in Fig. 7(*a*). Within the superspace formalism, this atom could be included in a different subsystem as in a commensurate composite crystal. Instead of that, it is more convenient to divide this O2 atom as indicated in Fig. 7(*a*), splitting it into two atomic domains, O2 and O3. The new O2 atomic domain becomes represented by a crenel function of width $\Delta = \Delta(\mathrm{Mo})$ located at $(\frac{1}{4}\frac{1}{4}0)$ and coordinate x_4^0 of its centre also given by equation (7). This atomic domain is also associated with Mo environments. The other segment forms the O3 atomic domain, located at the position $(\frac{1}{4}\frac{1}{4}\frac{1}{4})$ and represented by a crenel function with centre $x_4^0 = \frac{1}{2}$ and width $\Delta = 1 - \frac{\gamma}{2} - \Delta(\mathrm{Mo})$, where γ is the third component of the modulation vector. This O3 atom is related to the Bi coordination environments. Note that the t^0 parameter for the O2 atom can be determined considering t^0(O3) [which can be obtained from the application of equation (7)] and the widths of the crenel functions of O2 and O3 atoms. Thus, from Fig. 7(*b*) the parameter t^0(O2) is given by the expression

$$t^0(\mathrm{O2}) = t^0(\mathrm{O3}) - \frac{\Delta(\mathrm{O2}) + \Delta(\mathrm{O3})}{2}. \tag{9}$$

Note also that the calculation of the widths of the different atomic domains as functions of the width of the Mo atom allows the generalization of the model for any composition. As a consequence of the applied transformation to the superspace unit cell, the atomic domains obtained from the division of the O atoms in Fig. 7(*a*) present a linear positional modulation which can be described by the corresponding sawtooth functions. However, this displacive modulation can be neglected because only the average positions of the different atomic domains are interesting at this point. Therefore, the final atoms are represented by the corresponding crenel functions, obtaining the distribution indicated in Fig. 7(*b*).

A final step is required and consists of reducing the symmetry of the structure [given by the superspace group $X2cm(00\gamma)000$] maintaining only the twofold axis to obtain the corresponding monoclinic superspace group $F2(\alpha 0\gamma)$. In addition, a change of setting is required to work with the monoclinic axis along the **b** direction ($\mathbf{a}_{\mathrm{new}} = -\mathbf{b}_{\mathrm{old}}$, $\mathbf{b}_{\mathrm{new}} = \mathbf{a}_{\mathrm{old}}$, $\mathbf{c}_{\mathrm{new}} = \mathbf{c}_{\mathrm{old}}$).

The model obtained in this process corresponds to the $n = \infty$ compound (Aurivillius) using the basic cell of the fluorite structure and the modulation vector $\mathbf{q}_{\mathrm{F}} = \frac{2}{3}\mathbf{c}_{\mathrm{F}}^*$. An extrapolation of this model to the subject compounds is straightforward using the oblique modulation vector $\mathbf{q}_{\mathrm{o}}$ of equation (4). Note that for $n = \infty$ this vector reduces to the

Table 4
Atomic domains for the superspace model based on the Aurivillius-type structure of the compound Bi_2MoO_6.

According to the explained derivation, the superspace group of this model is $F2(\alpha 0\gamma)$, with the average unit cell defined by vectors $\{\mathbf{a}_{\mathrm{F}}, \mathbf{b}_{\mathrm{F}}, \mathbf{c}_{\mathrm{F}}\}$ and modulation vector given by equation (4).

Atom	Average position	t^0	x_4^0	Δ
Bi	(0 0 0)	$\frac{1}{2}$	$\frac{1}{2}$	$\frac{2(n+2)}{3n+4}$
Mo	(0 0 0)	0	0	$\frac{n}{3n+4}$
O1	$(00\frac{3}{8})$	0	equation (7)	$\frac{n}{3n+4}$
O2	$(\frac{1}{4}\frac{1}{4}0)$	$\frac{1}{2(3n+4)}$	equation (7)	$\frac{n}{3n+4}$
O3	$(\frac{1}{4}\frac{1}{4}\frac{1}{4})$	$\frac{n+2}{3n+4}$	$\frac{1}{2}$	$\frac{n+3}{3n+4}$
O4	$(\frac{1}{4}\frac{3}{4}\frac{1}{4})$	$\frac{n+2}{3n+4}$	$\frac{1}{2}$	$\frac{n+3}{3n+4}$

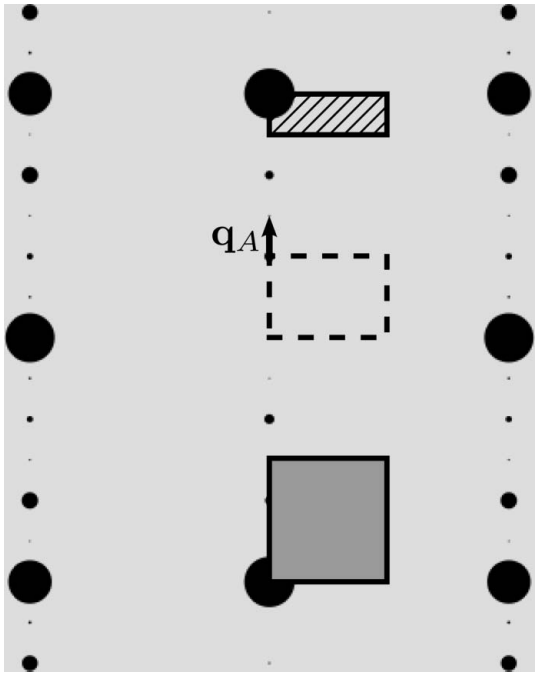

Figure 6
Weighted reciprocal space (0 *k l*) section of the diffraction pattern of the compound Bi_2MoO_6. This section is related to the (*h* 0 *l*) section of Fig. 1. Three different reciprocal unit cells can be observed, corresponding to the three-dimensional description (striped rectangle), the average structure of the superspace model for the Aurivillius family (dashed line) and the average unit cell based on fluorite structure (shaded rectangle). The modulation vector $\mathbf{q}_{\mathrm{A}}$ is also indicated.

value given above. Taking into account the formula of the system, $Bi_{2(n+2)}Mo_nO_{6(n+1)}$, the widths of the crenel functions for the Bi and Mo atoms can be given by $\frac{2(n+2)}{3n+4}$ and $\frac{n}{3n+4}$. Finally, the corresponding widths and t^0 parameters for O atomic domains can be derived as explained above. A description of the resulting model is presented in Table 4.

Since the studied compounds are commensurate, it is necessary to fix the value of the t parameter to determine the section of the superspace model which corresponds to the three-dimensional structure. The value $t = 0$ or its equivalents allow the recovery of a three-dimensional atomic distribution with a Mo atom located at a twofold axis. However, this t value leads to some problematic sections because some relevant points within the O2 and O3 or O2 and O4 atomic domains coincide with the ends of their crenel functions, connecting a single atom of the three-dimensional structure with two different atomic domains in the superspace model. This problem also appears in the application of this model to the $n = 5$ member. In both cases, these situations can be surmounted by slight modifications of the limits of the corresponding atomic domains, such that the global composition of the superspace model does not change.

Considering this superspace model, embedding of the refined three-dimensional structure of the $n = 3$ member has been carried out. In this case, when the ends of the O2 and O3 atoms coincide with a t-section, the O3 atomic domain has been decreased by a small quantity (δ) with the corresponding increase of the O2 atomic domain. In the same way as for O2 and O4 atoms the O4 atomic domain is slightly increased, and the O2 atomic domain is decreased. As a result of these modifications, the width of the crenel functions representing the O2 atom does not change, while the widths of the crenel functions for O3 and O4 atomic domains are $\frac{6}{13} - 2\delta$ and $\frac{6}{13} + 2\delta$. The resulting atomic domains are indicated in Table 5.

Table 5
Superspace model based on the Aurivillius structure for the member $n = 3$.

The superspace group is $F2(\alpha 0 \gamma)$ and the average unit cell is defined by vectors $\{\mathbf{a}_F, \mathbf{b}_F, \mathbf{c}_F\}$. The modulation vector is $\mathbf{q}_o = \frac{1}{13}(-2\mathbf{a}_F^* + 8\mathbf{c}_F^*)$.

Atom	Average position	t^0	x_4^0	Δ
Bi	(0 0 0)	$\frac{1}{2}$	$\frac{1}{2}$	$\frac{10}{13}$
Mo	(0 0 0)	0	0	$\frac{3}{13}$
O1	(0 0 $\frac{3}{8}$)	0	Equation (8)	$\frac{3}{13}$
O2	($\frac{1}{4}$ $\frac{1}{4}$ 0)	$\frac{1}{26}$	Equation (8)	$\frac{3}{13}$
O3	($\frac{1}{4}$ $\frac{1}{4}$ $\frac{1}{4}$)	$\frac{5}{13}$	$\frac{1}{2}$	$\frac{6}{13} - 2\delta$
O4	($\frac{1}{4}$ $\frac{3}{4}$ $\frac{1}{4}$)	$\frac{5}{13}$	$\frac{1}{2}$	$\frac{6}{13} + 2\delta$

In the above paragraphs the atomic domains have been established, but the real structure also includes positional modulation $\mathbf{u}(\bar{x}_4)$ for the atomic domains, which can be calculated from the embedding of the three-dimensional structure. Since the atoms are only defined within a limited region of the internal space their displacive modulations are expressed as a finite sum of some special functions

$$\mathbf{u}(\bar{x}_4) = \sum_n \mathbf{A}_n S_n(\bar{x}_4), \qquad (10)$$

where the special functions $S_n(\bar{x}_4)$ are orthogonalized harmonic functions for the Bi atom and Legendre polynomials for the rest of atoms. The parameters $\mathbf{A}_n$ of the modulation functions are determined by fitting the coordinates obtained in the embedding process to the corresponding functions. These parameters were checked through the refinement of the superspace model with the Rietveld method combining XPD and NPD data. Agreement between the observed and calculated patterns is almost the same as that achieved with the three-dimensional model (Fig. S1 of the supplementary material). Final reliability factors are presented in Table 2. Structural details as coordinates of the average structure, displacive modulation functions and displacement parameters are summarized in the deposited CIF file.

The resulting positional modulations of the different atomic domains are very wavy, especially for the O1 and O2 atoms. As an example, the posi-

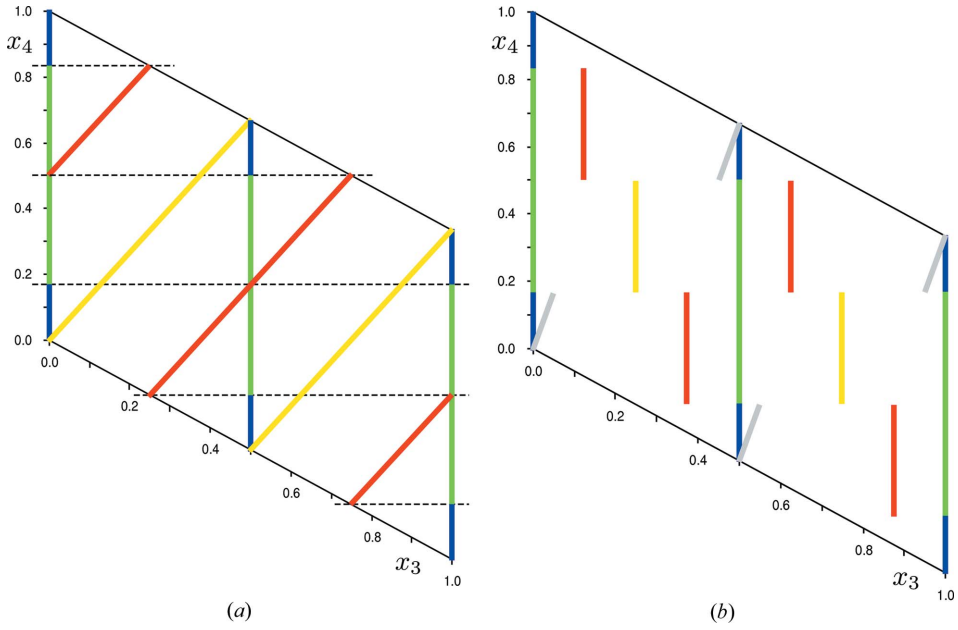

Figure 7
New description for the O1 (red) and O2 (yellow) atomic domains after the change of superspace unit cell (*a*). The *t*-sections associated with the ends of the cationic atomic domains are indicated (dashed lines). Oxygen atomic domains are divided considering these *t*-sections (*b*). Divided atomic domains without the linear positional modulation are shown: O1 (red), O2 (grey) and O3 (yellow). The O2 atomic domains are represented slightly oblique to avoid overlapping Mo atoms.

tional modulation along the z axis for the O atoms is represented in Fig. 8. In this case, the stronger distortions are exhibited by the O atomic domains associated with the environments of the Mo atoms, *i.e.* O1 and O2 atoms. However, O3 and O4 atoms, neighbours of Bi atomic domains, represent atoms which are not so scattered from their average position, which is $\frac{1}{4}$.

4. Member with n = 5

4.1. Refinement of the superspace model

The superspace model constructed above has been applied to build up the initial superspace model for the member $n = 5$ by substituting the composition-dependent parameter n in Table 4. The superspace group is $F2(\alpha 0\gamma)$, as for the $n = 3$ member, and the modulation vector is $\mathbf{q}_o = \frac{1}{19}(-2\mathbf{a}_F^* + 12\mathbf{c}_F^*)$, which is also derived from the general expression [equation (4)].

As in the case of the member with $n = 3$, fixing the value of the t parameter to $t = 0$ allows the recovery of the corresponding three-dimensional structure by establishing the relevant points of the atomic domains along the internal space. This three-dimensional model exhibits the expected cation distribution and a fairly accurate description of the O atoms associated with Bi cations. Only O atoms forming the environments of the Mo cations deviate from the expected structure, because Mo atoms should present tetrahedral coordination, whereas the developed superspace basic model leads to octahedral coordination instead. The transformation of this environment is achieved *via* the displacive modulation functions which distort the O1 and O2 atomic domains to reproduce the desired tetrahedral coordinations. As in the case of the member with $n = 3$, the displacive modulations of the different atoms are described as a truncated sum of special functions [equation (9)], employing orthogonalized harmonic functions for the Bi atom and Legendre polynomials for the other atomic domains.

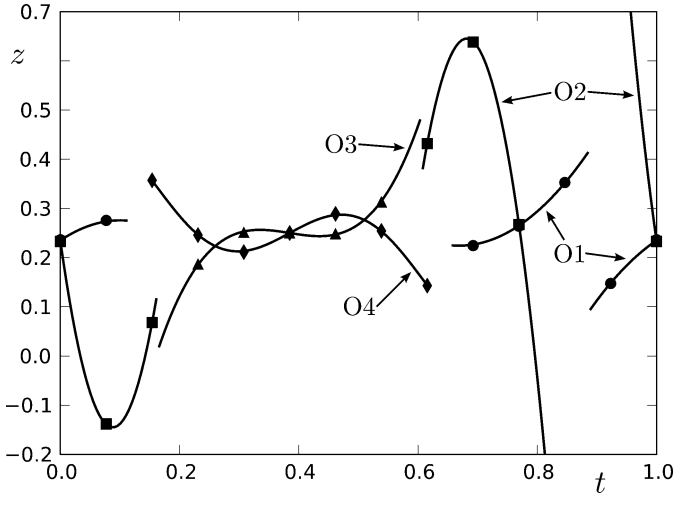

Figure 8
Positional modulation along the z coordinate for O1, O2, O3 and O4 atomic domains. Two additional atomic domains, symmetrically equivalent to O1 and O2 atoms, are also included. Continuous lines represent displacive modulations of atomic domains and the positions of atoms from a three-dimensional structure are indicated by discrete points. There are two overlapping points at different values of the t parameter ($t = 0, \frac{5}{13}, \frac{10}{13}$ and 1).

Within the superspace approach, the refinement of a modulated structure is usually a two-step process. Firstly, the average structure is refined using only the main reflections, and then the appropriate distortions are included into the model, refining the corresponding parameters. However, this approach is not adequate in this case, because the refined average structure is not a suitable intermediate structure since the coordination environments obtained for Mo atoms are far from tetrahedral. As an alternative, the parameters of the initial model are refined following certain order, established by the contribution of the different types of atoms to the XPD and NPD patterns. That is, first the parameters of the Bi atom, then the parameter of the Mo atom and finally the parameters of O atoms are refined. This refinement process leads to reasonable agreement with experimental data, obtaining a plausible model for the cations and O atoms associated with Bi atoms. However, the Mo cations exhibit unrealistic coordination environments and the inclusion of a restriction for the Mo—O distances does not improve this situation.

4.2. Refinement of the three-dimensional structure

To overcome the difficulties which arise in the refinement of the superspace model, a three-dimensional approach was used with special attention to the O atoms which form the environments of the Mo cations. The initial structure was constructed from the above described superspace model, considering only the cations and O atoms surrounded by Bi atoms. Ideal $\{MoO_4\}$ tetrahedra are introduced in the structure, trying to avoid too short O—O distances. This initial model is not complete since there are four missing O atoms, symmetrically equivalent, that will be included in a later stage of the refinement process at some of the positions indicated in Fig. 9. In the first stage, only x and z coordinates of the atoms are refined and in order to avoid some unreasonable Mo—O and O—O distances, some restrictions were introduced with values d(Mo—O) = 1.78 ± 0.01 Å and d(O—O) = 2.30 ± 0.01 Å. Distance restraints with larger sigma values do not produce any effect in the refinement process. Afterwards, a difference Fourier map was calculated, obtaining a peak which can be associated with the remaining O atom. Once the model has been completed, all atomic coordinates are refined, together with the isotropic temperature parameters, which have been grouped considering the different types of atoms and the similar positions that they occupy. The final agreement between observed and calculated patterns for both X-ray and neutron data sets is shown in Fig. S2 of the supplementary material and reliability factors are in Table 6. The final three-dimensional structure is represented in Fig. 10. Details of the refined structure (atomic coordinates, temperature factors, distances *etc.*) are summarized in the deposited CIF file.

Table 6
Background-corrected reliability factors obtained with the different models for XPD and NPD patterns of the $n = 5$ member.

	Three-dimensional model		Superspace model	
	XPD	NPD	XPD	NPD
R_p	0.1781	0.1430	0.1780	0.1427
R_{wp}	0.2138	0.1385	0.2137	0.1385
S	1.66	2.07	1.66	2.07
R_B(all)	0.0459	0.0678	0.0461	0.0673
R_F(all)	0.0298	0.0485	0.0300	0.0483
No. of parameters	103	99	105	101

4.3. Embedding of the three-dimensional structure

Once the three-dimensional structure of the $n = 5$ member has been refined, it is possible to carry out the embedding of the atomic distribution in order to calculate the parameters of the displacive modulations which could not be properly refined with the superspace model. Using the atomic domains derived from Table 4, each atom of the three-dimensional structure is associated with an average position. The atoms which correspond to the Bi, Mo, O3 and O4 atomic domains can be easily established. However, the remaining O atoms, which form the $\{MoO_4\}$ tetrahedra, cannot be clearly associated with any average position since the corresponding displacements are very large. There are several possible ways of establishing O1 and O2 atomic domains and this distribution is carried out trying to minimize the positional modulations.

After establishing the different atomic domains of the superspace model, parameters for their positional modulations $\mathbf{u}(\overline{x}_4)$ are calculated from the embedding. These parameters were checked by means of the refinement of the superspace structure through the Rietveld method, combining XPD and NPD data. The starting parameters hardly changed. Agreement between observed and calculated patterns is nearly the same as that obtained with the three-dimensional model (Fig. S2 of the supplementary material), with reliability factors presented in Table 6. Further details about the superspace model are enumerated in the deposited CIF file.

As in the case of the $n = 3$ member (Fig. 8), the positional modulation of the different atomic domains are very irregular, far from a simple linear or harmonic shape. As an example, the positional modulation along the z coordinate is represented for O atomic domains in Fig. 11. It can be observed that the strongest distortions are exhibited by the O atomic domains which define the tetrahedral O coordinations of the Mo atoms (O1 and O2). The atoms represented by O3 and O4 atomic domains, associated with Bi atoms, are not so spread out from their average positions with $z = \frac{1}{4}$. The large and irregular modulation functions of the O1 and O2 atomic domains explain why the refinement of the superspace model in the previous section is not successful, since O atoms which form the $\{MoO_4\}$ tetrahedra are located too far from their actual positions in the starting model.

5. Member with n = 4

5.1. Determination of the three-dimensional unit cell

The three-dimensional unit cell of this compound has been ambiguously determined, since two different values have been assigned to the lattice parameter a. In the first characterization of this compound Vila *et al.* (2004) proposed a value a = 29.0674 (5) Å, based on XPD data measured under high-resolution conditions in a diffractometer with a conventional X-ray source. On the other hand, a different parameter a' was suggested by Landa-Cánovas *et al.* (2009) with half the value of the previous one ($a' = \frac{a}{2}$). This new value is supported by a comparison of experimental and simulated HRTEM images, where the simulated images are obtained taking into account only cations. In fact, as shown by Fig. 12, the ideal f.c.c. cationic distribution assumed for this compound seems to indicate that the initially proposed unit cell can be described as twice the new one given by the vectors $\{\mathbf{a}', \mathbf{b}, \mathbf{c}\}$.

This new parameter a' is also apparently supported by the superspace model of the odd members when it is applied to $n = 4$. Using the modulation vector $\mathbf{q}_o = \frac{1}{16}(-2\mathbf{a}_F^* + 10\mathbf{c}_F^*)$ as derived from equation (4) for $n = 4$, it is easily shown that the vector $\mathbf{a}' = \frac{\mathbf{a}}{2}$ is a lattice vector of the three-dimensional commensurate superstructure. Or, in other words, the superspace model constructed above implies that the vectors

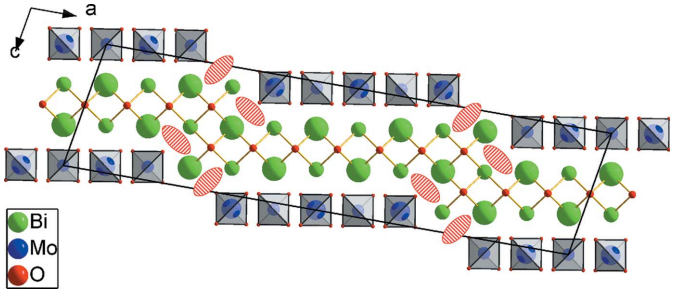

Figure 9
Projection along the **b** axis of the initial three-dimensional structure of the member with $n = 5$. Bi and Mo atoms are located at $y = 0$ (small spheres) and $y = \frac{1}{2}$ (large spheres). Missing O atoms can be located within the indicated regions (red ellipses).

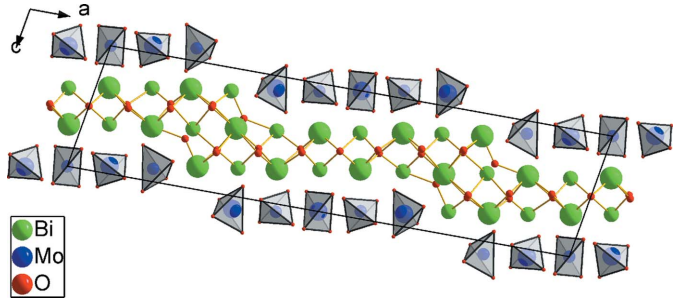

Figure 10
Projection along the **b** axis of the refined three-dimensional structure of the member with $n = 5$. Bi and Mo atoms are located at $y \simeq 0$ (small spheres) and $y \simeq \frac{1}{2}$ (large spheres).

$\{\mathbf{a}', \mathbf{b}, \mathbf{c}\}$ define a proper unit cell for the compound with $n = 4$.

However, in the XPD pattern obtained for the member $n = 4$ some reflections appear, indicated in Fig. 13, which cannot be indexed with this new unit cell. These reflections require the unit cell proposed by Vila *et al.* (2004) to be correctly indexed. Therefore, the unit cell given by the vectors $\{\mathbf{a}, \mathbf{b}, \mathbf{c}\}$ is the right one for the compound with $n = 4$, forcing the modification of the superspace model to obtain a valid unit cell for the three-dimensional structure recovered through a t-section.

5.2. Modification of the superspace model

Once the three-dimensional unit cell for the member $n = 4$ has been established it is possible to reinterpret the diffraction pattern to determine the average unit cell and the modulation vector. A schematic representation of the $(h\,0\,l)$ section of the diffraction pattern for the member $n = 4$ is shown in Fig. 14. According to the characterization carried out by Vila *et al.* (2004), this diffraction pattern presents the reflection condition $h\,0\,l$: $h = 2n$. Assuming this systematic extinction, neither $\mathbf{q}_o$ nor $\mathbf{q}_V$ (see Fig. 14) could be employed for correct indexing. Both modulation vectors allow the represented section $(h\,0\,l)$ to be indexed, but some Bragg peaks remain unindexed in other layers. In fact, the same set of reflections which cannot be indexed employing the vector $\mathbf{a}' = \frac{\mathbf{a}}{2}$ (Fig. 13) indicate that $\mathbf{q}_o$ and $\mathbf{q}_V$ are not suitable options for the superspace indexing. This problem is solved by choosing the modulation vector $\mathbf{q}_e = \frac{1}{16}(\mathbf{a}_F^* + 11\mathbf{c}_F^*)$, which allows the whole diffraction pattern to be indexed. This new modulation vector points to an extinction, as shown in Fig. 14. Note that with this modulation vector $\mathbf{q}_e$ the superspace model gives rise to the unit cell defined by the vectors $\{\mathbf{a}, \mathbf{b}, \mathbf{c}\}$ and the vector $\mathbf{a}' = \mathbf{a}/2$ is not a lattice vector.

The choice of modulation vector $\mathbf{q}_e$ implies the reflection condition $h\,0\,l\,m$: $m = 2n$, where n is an integer. This reflection condition points out two possible superspace groups: $F2/m(\alpha 0\gamma)0s$ or $Fm(\alpha 0\gamma)s$, selecting the centrosymmetric group as the first option. This group is equivalent to the standard group $B2/m(\alpha\beta 0)0s$ (No. 12.2 in Janssen *et al.*, 2004).

From the schematic representation of the electron diffraction (ED) pattern (Fig. 14), it is possible to obtain an expression for the new modulation vector in terms of the reciprocal vectors associated with the odd members superspace model

$$\mathbf{q}_e = \mathbf{c}_F^* - \frac{1}{2}\mathbf{q}_o. \tag{11}$$

Keeping the same unit cell for the average structure, the choice of this new modulation wavevector $\mathbf{q}_e$ implies a new superspace unit cell. As explained by Elcoro *et al.* (2003), the new vectors $\{\mathbf{a}'_{si}\}$ are given by the transformation

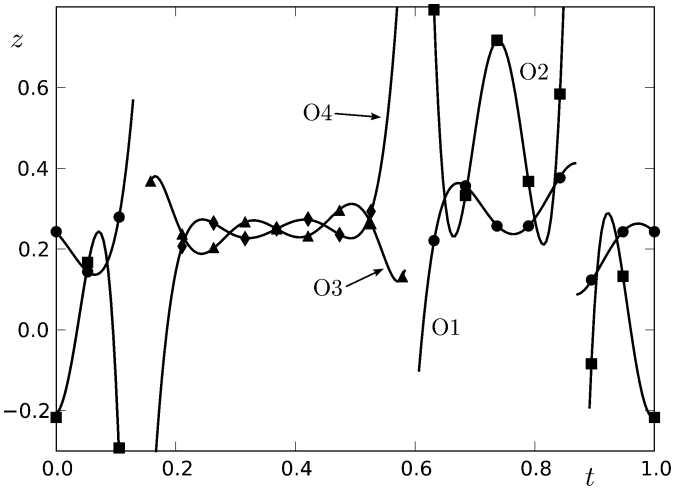

Figure 11
Positional modulation along the z coordinate for O1, O2, O3 and O4 atomic domains. Two additional atomic domains, symmetrically equivalent to O1 and O2 atoms, are also included. Continuous lines represent the positional modulation of atomic domains and positions of atoms from the three-dimensional structure are indicated by discrete points. There are two overlapping points at $t = \frac{7}{19}$.

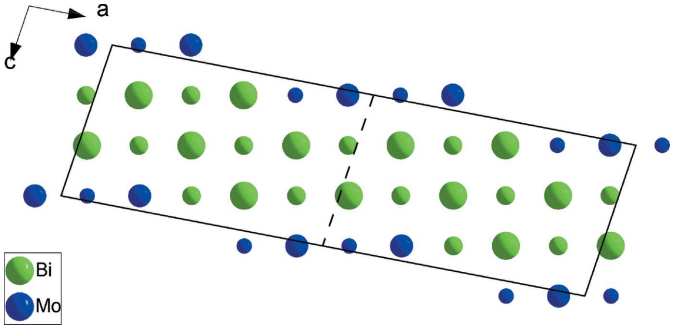

Figure 12
Projection along the **b** axis of the ideal three-dimensional cation distribution of the member with $n = 4$. Bi and Mo atoms are located at $y = 0$ (small spheres) and $y = \frac{1}{2}$ (large spheres). The first unit cell proposed (continuous line), defined by vectors $\{\mathbf{a}, \mathbf{b}, \mathbf{c}\}$, can be described as a duplication of the unit cell defined by vectors $\{\mathbf{a}', \mathbf{b}, \mathbf{c}\}$ (dashed line).

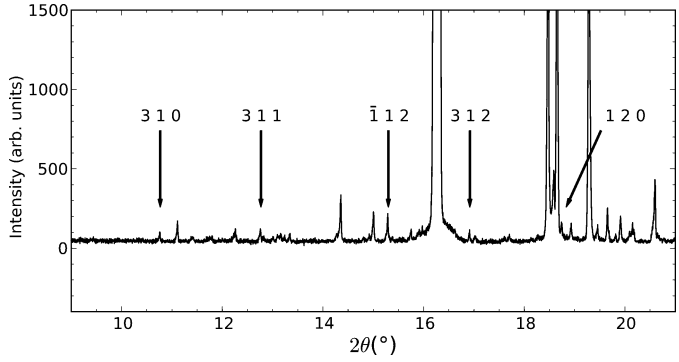

Figure 13
Detail of the XPD pattern of the $n = 4$ member. The indicated Bragg peaks are indexed with the vectors $\{\mathbf{a}, \mathbf{b}, \mathbf{c}\}$. Note that these reflections cannot be indexed using the vector $\mathbf{a}' = \mathbf{a}/2$.

Table 7
Possible values for the t parameter within the superspace model for the member $n = 4$.

The three-dimensional space groups corresponding to each t-section are indicated.

t value	$0 + \frac{k}{16}$	$\frac{1}{64} + \frac{k}{16}$	$\frac{1}{32} + \frac{k}{16}$	$\frac{3}{64} + \frac{k}{16}$	General
Space group	$P2/a$	$P2_1/a$	$P2/a$	$P2_1/a$	Pa

Table 8
Atomic distribution for the member $n = 4$ according to the model for odd members.

This description is associated with the superspace group $F2(\alpha 0\gamma)$. The unit cell of the average structure is given by vectors $\{\mathbf{a}_F, \mathbf{b}_F, \mathbf{c}_F\}$. The modulation vector of this model is $\mathbf{q}_o = \frac{1}{8}(-\mathbf{a}_F^* + 5\mathbf{c}_F^*)$.

Atom	Average position	t^0	x_4^0	Δ
Bi	(0 0 0)	$\frac{1}{2}$	$\frac{1}{2}$	$\frac{3}{4}$
Mo	(0 0 0)	0	0	$\frac{1}{4}$
O1	(0 0 $\frac{3}{8}$)	0	Equation (8)	$\frac{1}{4}$
O2	($\frac{1}{4}$ $\frac{1}{4}$ 0)	$\frac{1}{32}$	Equation (8)	$\frac{1}{4}$
O3	($\frac{1}{4}$ $\frac{1}{4}$ $\frac{1}{4}$)	$\frac{3}{8}$	$\frac{1}{2}$	$\frac{7}{16}$
O4	($\frac{1}{4}$ $\frac{3}{4}$ $\frac{1}{4}$)	$\frac{3}{8}$	$\frac{1}{2}$	$\frac{7}{16}$

$$\begin{pmatrix} \mathbf{a}'_{s1} \\ \mathbf{a}'_{s2} \\ \mathbf{a}'_{s3} \\ \mathbf{a}'_{s4} \end{pmatrix} = \begin{pmatrix} 1 & 0 & 0 & 0 \\ 0 & 1 & 0 & 0 \\ 0 & 0 & 1 & 2 \\ 0 & 0 & 0 & -2 \end{pmatrix} \begin{pmatrix} \mathbf{a}_{s1} \\ \mathbf{a}_{s2} \\ \mathbf{a}_{s3} \\ \mathbf{a}_{s4} \end{pmatrix}, \qquad (12)$$

where the vectors $\{\mathbf{a}_{si}\}$ correspond to the superspace unit cell of the odd members.

Note that with this change of unit cell, the superspace group $F2(\alpha 0\gamma)$ is transformed into the group $X2(\alpha 0\gamma)$, where X means non-standard centring vectors ($\frac{11}{22}00$), ($\frac{1}{2}0\frac{1}{2}0$), ($0\frac{11}{22}0$), ($000\frac{1}{2}$), ($\frac{11}{22}0\frac{1}{2}$), ($\frac{1}{2}0\frac{11}{22}$) and ($0\frac{111}{222}$). $X2(\alpha 0\gamma)$ and $F2/m(\alpha 0\gamma)0s$ are not group–subgroup related, but the former can be transformed into the latter by replacing the ($000\frac{1}{2}$) centring with a glide plane s given by $(x_1, -x_2, x_3, \frac{1}{2} + x_4)$.

As the three-dimensional structure is a commensurate superstructure of the basic unit cell, the corresponding t value is required. The different possibilities compatible with the superspace group $F2/m(\alpha 0\gamma)0s$ and the modulation vector $\mathbf{q}_e$ are enumerated in Table 7, where k is an arbitrary integer and a 'general' value of the t parameter refers to any value different from the others. Note that different choices of the t parameter can lead to different space groups for the resulting three-dimensional structure. The options $t = \frac{1}{64}$ and $t = \frac{3}{64}$ (and any of their equivalent values) lead to the centrosymmetric space group $P2_1/a$, as proposed by Galy *et al.* (2009). In fact, these two options are related through an origin shift ($\frac{11}{22}00$). Therefore, these two values are equivalent and $t = \frac{1}{64}$ is chosen. As in the superspace model for the odd members, this value of the t parameter means that some of the relevant points in the O2 and O3 atomic domains lie on the ends of their crenel functions (the value $t = \frac{3}{64}$ also leads to the same situation). This problem also apears in the application of this superspace model to the member $n = 6$. As explained above, this difficulty can be prevented by increasing slightly one of the atomic domains and decreasing the other one, without changing the global composition of the superspace model.

Using the general expressions from Table 4, the superspace model of the odd members applied for $n = 4$ can be derived, giving rise to the parameters shown in Table 8.

In this model the coordinate x_4^0 of the centre of the crenel functions for the O1 and O2 atomic domains are given by equation (7). Using the transformation of equation (11) and changing the symmetry from the superspace group $X2(\alpha 0\gamma)$ to the $F2/m(\alpha 0\gamma)0s$ group imply that the positions of the O3 and O4 atomic domains are merged into a unique one and the general position of O2 is split into two special positions at inversion centres (($\frac{1}{4}$, $\frac{1}{4}$, 0) and ($\frac{1}{4}$, $\frac{3}{4}$, 0)). The O atomic domains located at these special positions combined with the chosen parameter $t = \frac{1}{64}$ would give rise to O atoms placed at inversion centres in the three-dimensional structure. Each of these O atoms would be shared by two Mo cations which are symmetrically equivalent through the mentioned inversion centre. However, the expected environments for Mo cations are isolated tetrahedra without any shared O atoms. So these inversion centres cannot be occupied by any O atom and, therefore, O atomic domains cannot be located at these special positions in the superspace model. To obtain atomic domains more suitable for the expected Mo coordination, the two O atomic domains at special positions are replaced by one atomic domain at a general position, equidistant from both. The final superspace model is presented in Table 9. Note that after the transformation of equation (11) the widths of the crenel functions present half the previous value (Table 8). From Table 8, the coordinates x_4^0 of the centres of the O atomic

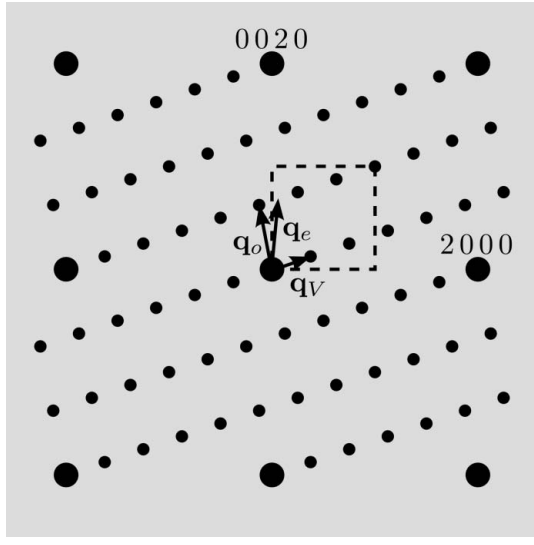

Figure 14
Schematic ($h\,0\,l$) section of the diffraction pattern of the member with $n = 4$. It corresponds to the ($h\,0\,l\,m$) section within the superspace approach. Main reflections ($m = 0$) are related to the reciprocal unit cell of the fluorite structure. The modulation vectors $\mathbf{q}_V$ and $\mathbf{q}_o$ allow this section to be indexed, but not the whole pattern. The indexing of the whole pattern is possible with the new modulation vector $\mathbf{q}_e$ and involves a reflection condition $h\,0\,l\,m:\ m = 2n$.

Table 9
Superspace model for the member n = 4.

This model is obtained through the modification of the superspace model for odd members. The superspace group is $F2/m(\alpha 0\gamma)0s$ with the average unit cell defined by vectors $\{\mathbf{a}_F, \mathbf{b}_F, \mathbf{c}_F\}$. The modulation vector is $\mathbf{q}_c = \frac{1}{16}(\mathbf{a}_F^* + 11\mathbf{c}_F^*)$.

Atom	Average position	x_4^0	t^0	Δ
Bi	(0 0 0)	$\frac{1}{4}$	$\frac{1}{4}$	$\frac{3}{8}$
Mo	(0 0 0)	0	0	$\frac{1}{8}$
O1	(0 0 $\frac{3}{8}$)	0	Equation (8)	$\frac{1}{8}$
O2	($\frac{1}{4}$ $\frac{1}{2}$ 0)	$-\frac{1}{64}$	Equation (8)	$\frac{1}{8}$
O3	($\frac{1}{4}$ $\frac{1}{4}$ $\frac{1}{4}$)	$-\frac{3}{16}$	Equation (8)	$\frac{7}{32}$

domains can be determined with equation (7). The transformation given by equation (11) is applied to the superspace coordinates $(\bar{\mathbf{r}}^0, x_4^0)$. These new coordinates are combined using equation (7) to obtain the t^0 values of Table 9.

The superspace model constructed above presents an ambiguity which deserves to be discussed. As presented in Table 9, Bi and Mo atomic domains are located in different special positions, implying certain restrictions. According to the superspace group of the proposed model, the Bi atomic domain is located at the special position (0 0 0 $\frac{1}{4}$) with twofold symmetry, while the Mo atomic domain is located at the special position (0 0 0 0) with inversion centre symmetry. They are different symmetries and, therefore, imply different restrictions on each atomic domain. However, there is no reason to discard a different configuration for the superspace model, with Bi and Mo atomic domains located at $x_4^0 = 0$ and $\frac{1}{4}$. This would correspond to an origin shift of the superspace group by the translation (000$\frac{1}{4}$) along internal space. Both configurations are acceptable and the only way to distinguish between them is to refine the structure of the compound.

Considering the value of the t parameter, a three-dimensional structure can be derived from the distribution of the atomic domains of Table 9. This three-dimensional model reproduces the expected distribution of the cations and approximate positions for the O atoms related to Bi cations. However, in this ideal model the O atoms which form the environments of the Mo cations are distributed in a different way than the expected one. These O atoms form square-planar coordination around Mo atoms, whereas the expected environments for these atoms are tetrahedral. In fact, as in the case of the model of the odd members, the O atoms which form the $\{MoO_4\}$ tetrahedra are located too far from their actual positions within the starting model. This is the reason why, to distinguish between the two possible configurations discussed above, it is more convenient to refine the structure of the $n = 4$ member through a three-dimensional approach, paying special attention to these O atoms.

5.3. Refinement of the three-dimensional structure

The procedure above leads to two configurations of the superspace model, depending on the position of the inversion centre relative to the atomic domain distribution. Each of these configurations corresponds to a different three-dimensional structure, because the cations are located at different positions with respect to the symmetry operations, although the ideal cation distribution is the same for both models. The two three-dimensional configurations are represented in Figs. 15(*a*) and (*b*). Note that in both cases the inversion centre of the space group $P2_1/a$ is located at the position (0 0 0) and the 2_1 screw axis at ($\frac{1}{4}$ *y* 0). Note also that, although Bi and Mo atomic domains are located at a twofold axis or an inversion centre within the superspace model, none of the Bi or Mo atoms are placed at special positions within the three-dimensional models. In fact, all the relevant points of the atomic domains, determined by the t parameter, are located at general positions.

The actual structure of the member $n = 4$ has been established through the refinement of these two possible three-dimensional models. The initial structures were derived from the superspace model presented in Table 9, including only cations and O atoms surrounded by Bi atoms. Ideal $\{MoO_4\}$ tetrahedra are introduced in the models avoiding too short O—O distances. This condition leads to different orientations of the tetrahedra for each model, as can be observed in Figs. 15(*a*) and (*b*) [models (I) and (II) respectively]. Each initial model lacks four symmetrically equivalent O atoms that were introduced during the refinement process at some of the indicated positions. The processes followed for the refinement of both models were similar to that described in the case of the

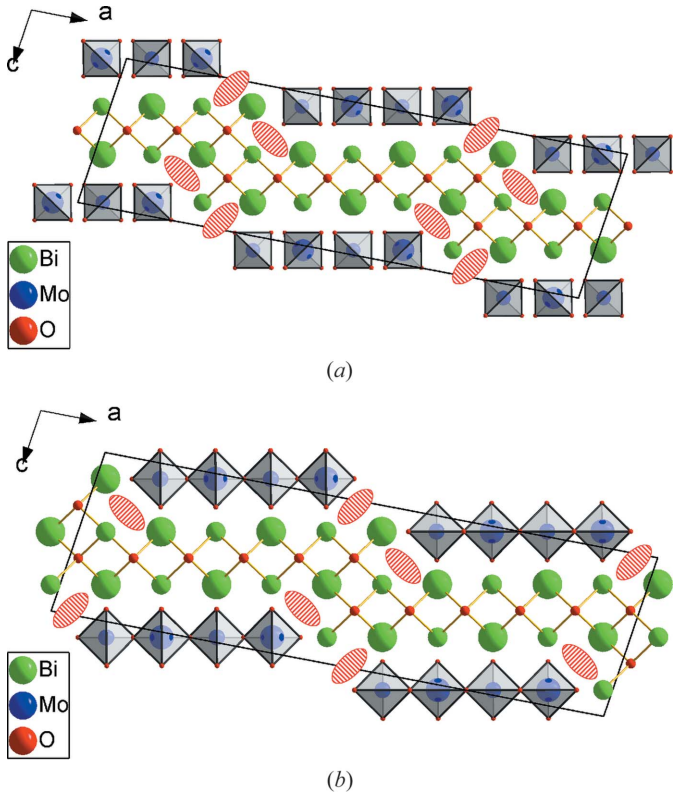

Figure 15
Projection along the **b** axis of the initial three-dimensional structures considered for the member with $n = 4$. Models (I) and (II) correspond to (*a*) and (*b*) respectively. Bi and Mo atoms are located at $y = \frac{1}{4}$ (small spheres) and $y = \frac{3}{4}$ (large spheres). Missing O atoms can be located within the indicated regions (red ellipses).

Table 10
Background corrected reliability factors obtained with the different models for XPD and NPD patterns of the n = 4 member.

	Three-dimensional model (I)		Three-dimensional model (II)		Superspace model	
	XPD	NPD	XPD	NPD	XPD	NPD
R_P	0.1433	0.1208	0.1575	0.1964	0.1431	0.1214
R_{wp}	0.1706	0.1174	0.1869	0.1875	0.1705	0.1182
S	1.33	1.65	1.46	2.61	1.33	1.66
R_B(all)	0.0336	0.0461	0.0453	0.1146	0.0334	0.0473
R_F(all)	0.0231	0.0371	0.0355	0.0863	0.0230	0.0379
No. of parameters	96	94	97	95	96	94

member with $n = 5$. Cations of the same type share the same displacement parameter, while O atoms are grouped depending on the different coordination environments to which they belong. The reliability factors obtained for both models are presented in Table 10 and point to model (I) as the correct one. Agreement between observed and calculated patterns (both X-ray and neutron data sets) is shown in Fig. S3 of the supplementary material, and the refined atomic distribution is represented in Fig. 16. Further details of the final three-dimensional structure, like atomic coordinates and isotropic temperature factors, are summarized in the deposited CIF file.

5.4. Embedding of the three-dimensional structure

After the refinement of the three-dimensional structure, the parameters of the displacive modulations $\mathbf{u}(\overline{x}_4)$ of the member $n = 4$ can be found through the embedding of the three-dimensional atomic distribution with a process similar to that developed for compounds with $n = 3$ and 5. From the displacements associated with each atom, it can be deduced that Bi and Mo atomic domains are located at a twofold axis and an inversion centre, respectively, thus resolving the ambiguity which arises in the construction of the superspace model. The configuration indicated in Table 9 is the correct one. As in the case of members $n = 3$ and 5, the atoms of the model are only defined within a limited region of internal space. Therefore, their positional modulations $\mathbf{u}(\overline{x}_4)$ are expressed as a finite sum of some special functions [see equation (9)]. The special functions $S_n(\overline{x}_4)$ used are orthogonalized harmonic functions for the Bi atom and Legendre polynomials for the others. The superspace model thus obtained was checked through the Rietveld method combining XPD and NPD data. Agreement between observed and calculated patterns is similar to that obtained with the three-dimensional model (Fig. S3 in the supplementary material) and reliability factors are presented in Table 10. More details on the superspace model are given in the CIF file.

As for members $n = 3$ and 5, the O atoms of the superspace model also exhibit strong displacive modulations. As an example, positional modulation along the z axis for O atomic domains is shown in Fig. 17. The atomic domains associated with the Mo coordination, *i.e.* O1 and O2 atoms, present the largest distortions. In contrast, the O3 atomic domain represents atoms which are not so scattered from their average position ($\sim \frac{1}{4}$)

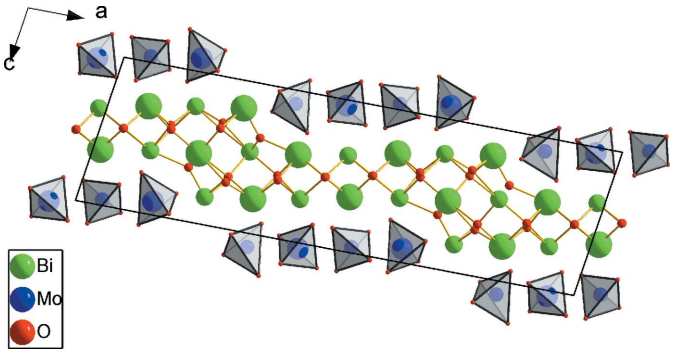

Figure 16
Projection along the **b** axis of the refined three-dimensional structure of the member $n = 4$ corresponding to the initial structure given by model (I) (Fig. 15*a*). Bi and Mo atoms are located at $y \simeq \frac{1}{4}$ (small spheres) and $y \simeq \frac{3}{4}$ (large spheres).

6. Member with n = 6

The superspace model constructed for the compound with $n = 4$ can be easily generalized to any even member of the family. To this aim, the general expressions for widths of atomic domains and modulation vectors have been determined, keeping the same superspace group $F2/m(\alpha 0\gamma)0s$. The

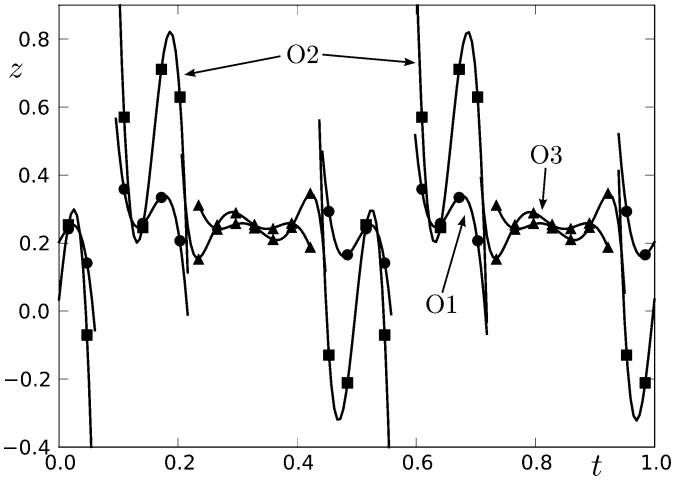

Figure 17
Positional modulation along the z coordinate for O1, O2 and O3 atoms. Several symmetrically equivalent atomic domains have been included. Coordinates of atoms from the three-dimensional structure are indicated by discrete points. Continuous lines represent displacive modulations of atomic domains. There are two overlapping points at different values of the t parameter ($t = \frac{1}{64}, \frac{9}{64}, \frac{17}{64}, \frac{21}{64}, \frac{25}{64}, \frac{33}{64}, \frac{41}{64}, \frac{49}{64}, \frac{53}{64}$ and $\frac{57}{64}$).

relationship between the superspace unit cells of odd and even members [equation (11)] establishes that the widths of the atomic domains for an even model are half of the corresponding values for the odd members (see Table 4). Expressions for general values of atomic domains are in Table 11. The coordinates and t^0 parameters were obtained as in the case of the member with $n = 4$. From equation (10) and the general expression for the modulation vector $\mathbf{q}_o$ [equation (4)], the generalization of the modulation vector $\mathbf{q}_e$ can be calculated, leading to

$$\mathbf{q}_e = \frac{1}{3n+4}(\mathbf{a}_F^* + (2n+3)\mathbf{c}_F^*). \qquad (13)$$

6.1. Refinement of the superspace model

An initial superspace structure for the $n = 6$ member can be obtained from the general model constructed above for even members. The superspace model is based on the superspace group $F2/m(\alpha 0\gamma)0s$, with $\mathbf{q}_e = \frac{1}{22}\mathbf{a}_F^* + \frac{15}{22}\mathbf{c}_F^*$ and atomic domains obtained from Table 11 with $n = 6$.

Once the superspace group and modulation vector have been established, the value of the t parameter is determined as in the case of the member $n = 4$. Table 12 resumes the different space groups arising from the possible t values. Among them, the value $t = \frac{1}{88}$ or equivalent ones is the most suitable according to the same arguments explained for the compound with $n = 4$.

The three-dimensional structure obtained from the superspace model of this compound and the refinement process of this model present the same problems which have been explained in the case of members $n = 5$ and 4.

6.2. Refinement of the three-dimensional structure

In order to obtain the positions of the O atoms which cannot be determined through the superspace approach, the refinement of the three-dimensional structure was carried out as previously explained for the remaining compounds of the system. The initial three-dimensional structure is indicated in Fig 18. To avoid unreasonable Mo—O distances, some restrictions were introduced with values d(Mo—O) = 1.79 ± 0.01 Å. Isotropic temperature parameters were refined for all atoms, with a different parameter associated with each type of atom. However, the displacement parameters of Mo and O atoms became negative after the refinement process, and they were fixed to the value U_{iso} = 0.02 Å^2. The obtained agreement between observed and calculated XPD and NPD is shown in Fig. S4 of the supplementary material, with reliability factors given in Table 13. The final three-dimensional structure obtained for the member $n = 6$ is represented in Fig. 19. Further details on this structure are given in the deposited CIF file.

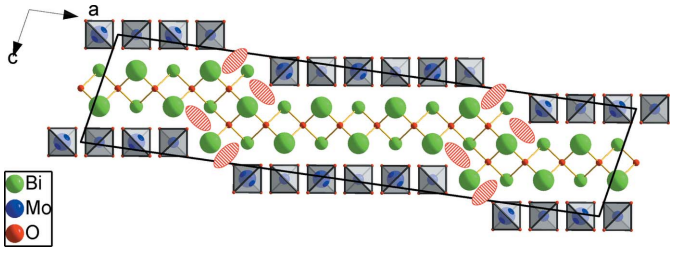

Figure 18
Projection along the **b** axis of the initial three-dimensional structure of the member with $n = 6$. Bi and Mo atoms are located at $y = \frac{1}{4}$ (small spheres) and $y = \frac{3}{4}$ (large spheres). Missing O atoms can be located within the indicated regions (red ellipses).

Table 11
Superspace model for even members.

The superspace group of this model is $F2/m(\alpha 0\gamma)0s$, and the unit cell of the average structure is determined by vectors $\{\mathbf{a}_F, \mathbf{b}_F, \mathbf{c}_F\}$. The modulation vector is given by equation (13).

Atom	Average position	t^0	x_4^0	Δ
Bi	(0 0 0)	$\frac{1}{4}$	$\frac{1}{4}$	$\frac{n+2}{3n+4}$
Mo	(0 0 0)	0	0	$\frac{n}{2(3n+4)}$
O1	(0 0 $\frac{3}{8}$)	0	Equation (8)	$\frac{n}{2(3n+4)}$
O2	($\frac{1}{4}$ $\frac{1}{2}$ 0)	$-\frac{1}{4(3n+4)}$	Equation (8)	$\frac{n}{2(3n+4)}$
O3	($\frac{1}{4}$ $\frac{1}{4}$ $\frac{1}{4}$)	$-\frac{n+2}{2(3n+4)}$	Equation (8)	$\frac{n+3}{2(3n+4)}$

Table 12
Possible values for the t parameter within the superspace model for the member n = 6.

The three-dimensional space groups corresponding to each t-section are indicated.

t value	$0+\frac{k}{22}$	$\frac{1}{88}+\frac{k}{22}$	$\frac{1}{44}+\frac{k}{22}$	$\frac{3}{88}+\frac{k}{22}$	General
Space group	$P2/a$	$P2_1/a$	$P2/a$	$P2_1/a$	Pa

6.3. Embedding of the three-dimensional structure

After obtaining the three-dimensional structure of the $n = 6$ member, the parameters of the displacive modulations of the superspace model can be determined through the embedding of the three-dimensional atomic distribution. The procedure is similar to that described for the previous compounds. Once the atomic domains of the superspace model have been determined, the corresponding parameters of their displacive modulations $\mathbf{u}(\bar{x}_4)$ can be calculated by fitting the atomic displacements to the corresponding sum of functions [equation (9)]. The resulting parameters were checked by refining them through the Rietveld method using XPD and NPD data. Agreement obtained between observed and calculated patterns is similar to that obtained with the three-dimensional model (Fig. S4 in the supplementary material). The reliability factors are presented in Table 13. The results are summarized in the deposited CIF file.

As in the remaining members of the family, the different atomic domains exhibit very irregular positional modulations, without simple linear or harmonic functions. As an example, the displacive modulation of O atomic domains along z is represented in Fig. 20.

Table 13
Background-corrected reliability factors obtained with the different models for XPD and NPD patterns of the $n = 6$ member.

The peaks of the XPD pattern present anisotropic strain broadening which has been corrected through the tensor method. The formulation of this correction is different for the three-dimensional and the superspace models. The superspace formulation of this correction implies more parameters. This is the origin of these different R values.

	Three-dimensional model		Superspace model	
	XPD	NPD	XPD	NPD
R_p	0.1550	0.1492	0.1446	0.1449
R_{wp}	0.1970	0.1416	0.1848	0.1384
S	1.74	1.78	1.65	1.76
R_B	0.0471	0.0597	0.0436	0.0575
R_F	0.0361	0.0515	0.0318	0.0475
No. of parameters	127	112	137	112

7. Discussion and conclusion

In the referenced examples of systems with flexible composition (Evain *et al.*, 1998; Perez-Mato *et al.*, 1999; Elcoro *et al.*, 2000, 2001), each family is described within the superspace formalism by a unique model. A common average structure combined with a composition-dependent modulation vector represents the structure of each compound of the series. In the case of the series $Ca_n(Nb,Ti)_nO_{3n+2}$ (Guevarra *et al.*, 2007), even the modulation functions of different members of the system ($n = 5$ and 6) are comparable. However, in the present study of the family $Bi_{2(n+2)}Mo_nO_{6(n+1)}$ two superspace models are required. The odd members of the family are described with a superspace model and the even members with another one. As explained above, each model exhibits its own superspace group and its own general expressions for modulation vectors and widths of the atomic crenel functions. Nevertheless, both models are not so different and present features which are similar. The average structures are comparable and the occupational modulation for cations in the even members model can be considered as a duplication along internal space of the corresponding occupational modulation in the odd model.

In both cases, the superspace models make visible the relation between the structure and the composition for the different compounds of this family. On the one hand, the n parameter determines the composition of each member of the series. On the other, this parameter is also present in the general expressions of modulation wavevectors, which determines the three-dimensional supercell of the corresponding compound.

Moreover, the application of superspace formalism to this family of compounds shows both the possibilities and limitations of this approach. Thus, cations and O atoms associated with Bi environments can be described quite well within superspace formalism. In particular, the cationic distribution of each compound is represented in a rather concise way, through complementary crenel functions whose widths depend on the composition parameter n. On the other hand, it is not straightforward to describe the spatial distribution of the O atoms forming $\{MoO_4\}$ tetrahedra through an average position and the corresponding distortion. Actually, these O atomic domains exhibit very large and irregular displacive modulations. In fact, the ideal structure generated by the superspace model considering only occupational modulation gives rise to environments for Mo atoms which are far from the actual ones for these cations, consisting of isolated tetrahedra. In this sense, the developed superspace models can be considered an extreme case of the application of the superspace formalism to describe a system of flexible composition as a modulated structure with a composition-dependent modulation wavevector.

Obviously, an important objection to the presented superspace models could be that, without the inclusion of positional modulations for some O atoms, these models do not lead to isolated $\{MoO_4\}$ tetrahedra in the resulting three-dimensional structure. An *ideal* superspace model should generate this type of Mo environment directly. Clearly, this *ideal* model has

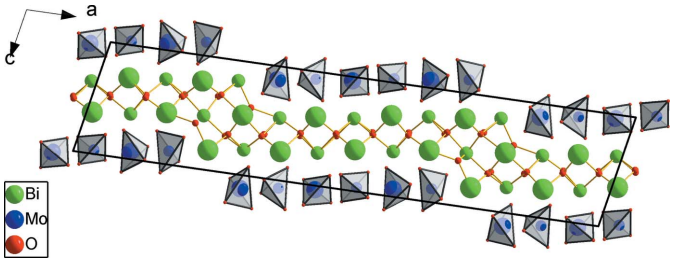

Figure 19
Projection along the **b** axis of the refined three-dimensional structure of the $n = 6$ member. Bi and Mo atoms are located at $y \simeq \frac{1}{4}$ (small spheres) and $y \simeq \frac{3}{4}$ (large spheres).

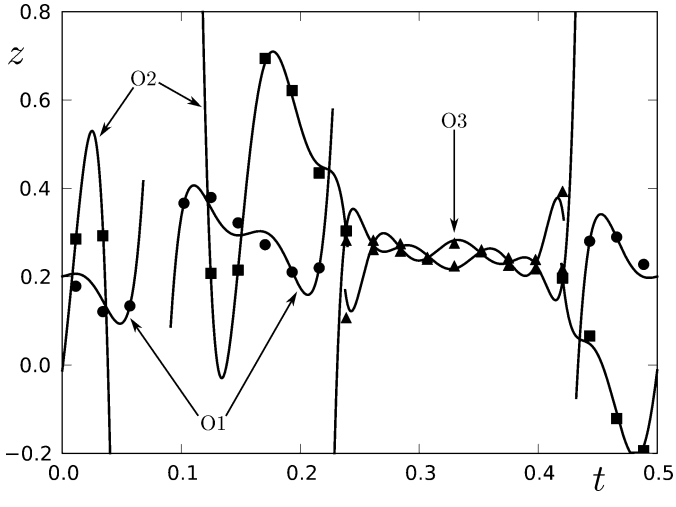

Figure 20
Positional modulation along the z coordinate for O1, O2 and O3 atomic domains. Some symmetrically equivalent atomic domains are indicated. Continuous lines represent the positional modulation of atomic domains and positions of atoms from the three-dimensional structure are indicated by discrete points. There are two overlapping points at $t = \frac{27}{88}$ and $\frac{31}{88}$. The interval from $t = 0.5$ to $t = 1$ is very similar to that presented in the figure according to the glide plane $(x_1, -x_2, x_3, \frac{1}{2} + x_4)$.

not been achieved. In fact, neither the possibility nor the impossibility of such a model can be assured. Instead, the Mo environments obtained from the odd and even superspace models (without displacive modulations) are corner-sharing octahedra and square planar, respectively. This is a consequence of the approach followed in the present work. The superspace model for odd members has been constructed taking as reference the Aurivillius structure of the compound Bi_2MoO_6. The corner-sharing octahedra are a legacy of the octahedral layers of this Aurivillius structure. Also the planar square environments within the even members model are a result of the modification of the odd members superspace model.

Another doubtful question concerning the present work could be the necessity of constructing two different superspace models. Even two different modulation vectors ($\mathbf{q}_o$ and $\mathbf{q}_e$) are required. Thus, the modulation vector of the odd model ($\mathbf{q}_o$) does not allow the diffraction pattern of even compounds to be indexed. Also the modulation vector of the even model ($\mathbf{q}_e$) does not lead to the correct three-dimensional space group when used with the odd members. In fact, the construction of a general model for both odd and even members of this family is an open question whose resolution would require further investigations.

One advantage of these superspace models is that they do not present any restriction for the n parameter included in the expressions of the general models. Although only members with $n = 3$, 4, 5 and 6 have been synthesized, the proposed models could be applied to any value of the n parameter. That is, the obtained models also provide an ideal structural model for those compounds of the family which have not been synthesized, even for compounds with a non-integer n parameter.

As explained above, the superspace models proposed for the family $Bi_{2(n+2)}Mo_nO_{6(n+1)}$ are based on the Aurivillius-type structure of the compound Bi_2MoO_6, which is one of the end members of the system (with $n = 0$). As shown in the supplementary material, an alternative superspace model could be constructed from the fluorite-like structure of the compound δ-Bi_2O_3 (the other end member of the system, with $n = 0$). In fact, they present the same description for the cations of the structure and the distinction between these two models consists of a different description of the O atoms. In the case of the model based on the fluorite-type structure, two atomic domains represent all O atoms and both include O atoms associated with Bi and Mo cations. Thus, O atoms related with very different coordination environments are associated with the same average position. Meanwhile, the model based on the Aurivillius structure describes the O atoms of each compound by means of four different atomic domains, which do not mix atoms related with environments of Bi and Mo cations. In other words, the O atoms related to different coordination environments are associated with different average positions. Therefore, the model based on the Aurivillius structure appears to be more suitable since this model leads to two different coordination environments, which is a feature exhibited by this family of compounds.

In conclusion, the superspace formalism has been applied to the description of the $Bi_{2(n+2)}Mo_nO_{6(n+1)}$ system. Two models have been proposed, each one corresponding to the members with different parity of n. The model constructed for odd members of this family cannot be applied to the even members since it does not lead to a correct three-dimensional unit cell for the even members. Therefore, the odd members model is modified to obtain a superspace model for the even members of the family. The corresponding superspace models for the different compounds of the system have been checked through the Rietveld method combining XPD and NPD data. In all the compounds of this family the O atoms related to the $\{MoO_4\}$ tetrahedra exhibit very strong displacive modulations.

The authors are grateful to J. Galy, A. R. Landa-Cánovas and J. Hernández-Velasco for their helpful discussions. This work was supported by the Basque Government (project IT-282-07). This work was also supported by the European Community Research Infrastructure Action under the FP6: 'Structuring the European Research Area' ['Integrating Activity on Synchrotron and Free Electron Laser Science' (IA-SFS) RII3-CT-2004-506008]. PJB also thanks the Basque Government for financial support.

References

Agarwal, D. D., Madhok, K. L. & Goswami, H. S. (1994). *React. Kinet. Catal. Lett.* **52**, 225–232.
Boullay, P., Trolliard, G., Mercurio, D., Perez-Mato, J. M. & Elcoro, L. (2002*a*). *J. Solid State Chem.* **164**, 252–260.
Boullay, P., Trolliard, G., Mercurio, D., Perez-Mato, J. M. & Elcoro, L. (2002*b*). *J. Solid State Chem.* **164**, 261–271.
Elcoro, L., Perez-Mato, J. M., Darriet, J. & El Abed, A. (2003). *Acta Cryst.* B**59**, 217–233.
Elcoro, L., Perez-Mato, J. M. & Withers, R. L. (2000). *Z. Kristallogr.* **215**, 727–739.
Elcoro, L., Perez-Mato, J. M. & Withers, R. L. (2001). *Acta Cryst.* B**57**, 471–484.
Elcoro, L., Zúñiga, F. J. & Perez-Mato, J. M. (2004). *Acta Cryst.* B**60**, 21–31.
Elzen, A. F. van den & Rieck, G. D. (1973). *Acta Cryst.* B**29**, 2433–2436.
Evain, M., Boucher, F., Gourdon, O., Petříček, V., Dušek, M. & Bezdicka, P. (1998). *Chem. Mater.* **10**, 3068–3076.
Galvan, D. H., Fuentes, S., Avalos-Borja, M., Cota-Araiza, L., Early, E. A., Maple, M. B. & Cruz-Reyes, J. (1993). *J. Phys. Condens. Matter*, **5**, A217–A218.
Galy, J., Hernández-Velasco, J., Landa-Cánovas, A. R., Vila, E. & Castro, A. (2009). *J. Solid State Chem.* **182**, 1177–1187.
Galy, J., Salles, P., Rozier, P. & Castro, A. (2006). *Solid State Ionics*, **177**, 2897–2902.
Guevarra, J., Schönleber, A., van Smaalen, S. & Lichtenberg, F. (2007). *Acta Cryst.* B**63**, 183–189.
Holmes, L., Peng, L., Heinmaa, I., O'Dell, L. A., Smith, M. E., Vannier, R. N. & Grey, C. P. (2008). *Chem. Mater.* **20**, 3638–3648.

Janssen, T., Janner, A., Looijenga-Vos, A. & de Wolff, P. (2004). *International Tables for Crystallography*, 3rd ed., pp. 907–945. Dordrecht: Kluwer Academic Publishers.
Landa-Cánovas, Á. R., Vila, E., Hernández-Velasco, J., Galy, J. & Castro, A. (2009). *Acta Cryst.* B**65**, 458–466.
Perez-Mato, J. M., Zakhour-Nakhl, M., Weill, F. & Darriet, J. (1999). *J. Mater. Chem.* **9**, 2795–2808.
Petříček, V., Dušek, M. & Palatinus, L. (2006). *JANA*2006. Institute of Physics, Praha, Czech Republic.
Vannier, R. N., Danzé, S., Nowogrocki, G., Huvé, M. & Mairesse, G. (2000). *Solid State Ionics*, **136–137**, 51–59.
Vila, E., Iglesias, J. E., Galy, J. & Castro, A. (2005). *Solid State Sci.* **7**, 1369–1376.
Vila, E., Landa-Canovas, A. R., Galy, J., Iglesias, J. E. & Castro, A. (2007). *J. Solid State Chem.* **180**, 661–669.
Vila, E., Rojo, J. M., Iglesias, J. E. & Castro, A. (2004). *Chem. Mater.* **16**, 1732–1739.